Memoirs of the Faculty of Engineering, Nagoya University
Vol. 37, No. 1 (1985)

THEORETICAL AND EXPERIMENTAL STUDIES IN CAKE FILTRATION

MOMPEI SHIRATO, MASAO SAMBUICHI*,
TOSHIRO MURASE, TSUTOMU ARAGAKI,
KAZUMASA KOBAYASHI** and EIJI IRITANI

Department of Chemical Engineering

(Received May 21, 1985)

Abstract

Filtration of liquid suspensions is a widely practiced process in many industries. While a substantial number of investigators have made valuable contributions to the literature, experimentation still plays the essential role in the prediction of filtration characteristics, particularly when compressible cakes are involved. In an actual filtration, both the flow rate of liquid and migration rate of solids vary throughout the cake. The internal flow variations in filter cakes have a significant effect on the observed filtration behavior when the feed slurries are highly concentrated.

Taking variable flow rates of liquid and solid into accont, the so-called modern filtration theory is developed. Validity of the theory is examined by considering experimental variation of porosity and hydraulic pressure within the filter cake. Characteristics of constant pressure, constant rate and variable pressure-variable rate filtrations can be accurately predicted on the basis of compression-permeability cell data corrected for cell-wall friction. In view of the effective filtration area factor, non uni-dimensional filtration problems can be solved in an analogous manner to conventional uni-dimensional problems. The generalized filtration theory which can be applied to both Newtonian and non-Newtonian fluids is developed on the basis of the power-law model for non-Newtonian fluids.

* Department of Chemical Engineering, Yamaguchi University
** Department of Chemical Engineering, Gunma University

CONTENTS

Introduction

Filtration is the operation of separating a dispersed phase of solid particles from a fluid by means of a filter medium which permits the passage of the fluid but retains the particles. Such filtration steps are required in many important processes and in widely divergent industries. In recent years, the importance of filtration techniques has been emphasized by the increased need for protection of the environment and by the increasingly critical need for larger supplies of energy.

The overall concept of Ruth's average specific filtration resistance[1] has long played a central role in the development of filtration theories and experimental works. This concept, however, shed little light on the internal mechanisms of cake filtration operations nor properly explained many of the specific problems encountered in industry. Investigation of local cake conditions as controlling the overall filtration resistance began with the theoretical and experimental developments by Grace,[2,3] Tiller,[4,5] Ingmanson,[6] Kottwitz and Boylan,[7] and Okamura and Shirato,[8,9] while Carman,[10,11] and Ruth[12] introduced the compression-permeability technique for theoretical analysis of filtration. Starting from an analytical study of the internal filtration mechanisms, the so-called modern filtration theory has been developed.[13~15]

The principal objective of this paper is to present logical analytical methods for practical filtration operations on the basis of the modern filtration theory which involves variable flow rates through filter cake. This paper is composed of seven chapters. Chapter 1 presents several important notes on the overall filter cake characteristics.[16,17] Chapter 2 deals with the internal flow mechanisms in filter cakes under constant pressure conditions.[8,13~15] Taking the variations of both the flow rate of liquid and the migration rate of solids into account, the so-called modern filtration theory is developed. Chapter 3 is related to the compression-permeability test method which is worthwhile for the analysis of internal flow mechanisms through compressible porous beds.[9] Limitations of the compression-permeability cell are also discussed.[18~20] Chapter 4 is concerned with experimental verification of modern filtration theory.[19,20] The theory is verified by direct measurements of porosity variations through cakes by using an electrical method. Chapter 5 deals with constant rate and variable pressure-variable rate filtration operations which are the most important in the process industries.[18,21] Chapter 6 presents analytical methods for calculating non uni-dimensional filtration.[22~25] Non uni-dimensional filtration problems can be solved in view of effective filtration area factor. Chapter 7 is concerned with non-Newtonian filtration of power-law fluids.[26~30] The generalized filtration theory which can be applied to both Newtonian and non-Newtonian fluids is developed.

1. Overall Filter Cake Characteristics

The overall filter cake characteristics have hitherto been discussed on the basis of the so-called Ruth's filtration theory[31]. The conventional Ruth's filtration rate equation is given by

$$\frac{1}{q_1}\equiv\frac{d\theta}{dv}=\frac{2}{K}(v+v_m) \tag{1.1}$$

where q_1 is the filtration velocity, θ the filtration time, v the filtrate volume per unit area, v_m the fictitious filtrate volume per unit area, equivalent to medium resistance, and K the Ruth coefficient of constant pressure filtration defined by

$$K\equiv\frac{2p(1-ms)}{\mu\alpha_{av}\rho s} \tag{1.2}$$

where p is the applied filtration pressure, m the mass ratio of wet to dry cake, s the mass fraction of solid in the slurry, μ the filtrate viscosity, ρ the filtrate density, and α_{av} the average specific filtration resistance. Equation (1.1) is frequently the starting point for the development of filtration equations. It serves as the basis for interpreting test data carried out at constant pressure.

On the assumption that K is constant in a constant pressure filtration, integration of Eq. (1.1) results in

$$(v+v_m)^2=K(\theta+\theta_m) \tag{1.3}$$

where θ_m is the fictitious filtration time corresponding to the medium resistance. Equation (1.3) is simply the equation of the well-known filtration parabola.

In the papers previously published by several other authors,[32,33] α_{av} for constant pressure filtration was represented as a function of a single variable, that is, the filtration pressure p. According to the results of our constant pressure filtration experiments with the so-called ceramic slurries, the ignition-plug slurry is the only case where α_{av} is a function of a single variable p; for all other slurries, the dependence of α_{av} is more complex.[16]

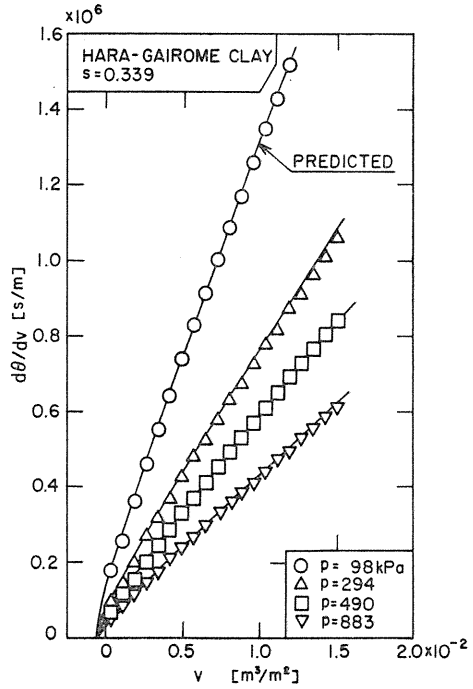

Fig. 1. 1. Relation between $d\theta/dv$ and v.

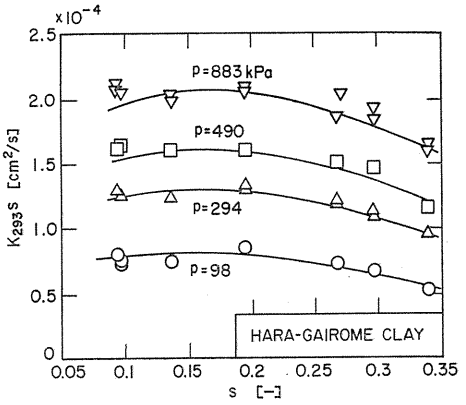

Fig. 1. 2. Effect of s on $K_{293}s$.

Figure 1. 1 illustrates the experimental results of $d\theta/dv$ vs. v of Gairome Clay slurries during constant pressure filtration. The $d\theta/dv$ vs. v relation indicates a curve, which approaches asymptotically to a straight line as v increases. The value of K can be determined from the slope of the straight portion of $d\theta/dv$ vs. v on

the basis of Eq. (1.1). Ruth coefficient at 293K, K_{293}, can be calculated from

$$K_{293}\mu_{293}=K\mu \tag{1.4}$$

where μ_{293} is the viscosity of filtrate at 293K.

In Fig. 1. 2, plots of $K_{293}s$ vs. s are shown. The behavior of $K_{293}s$ vs. s for each constant pressure filtration case tends to be curved convexly upwards. It is expected that α_{av} is a function of s as well as of p.

In Fig. 1. 1 $d\theta/dv$ vs. v deviates from the linear relationship at the beginning of the filtration. It then follows that α_{av} is a function not only of p and s but also of v. Using Eqs. (1.1) and (1.2) and applying the m-values predicted on the basis of the compression-permeability data to the constant pressure filtration results, the following empirical equation of α_{av} is obtained:

$$\begin{aligned}\alpha_{av}&=\alpha_{app}+\alpha_{corr}\\&=8.37\times10^{8}p^{0.60}s^{-0.38}+2.85\times10^{7}sp^{0.60}v^{-2/3}\end{aligned} \tag{1.5}$$

Therefore, the average specific resistance, α_{av}, of the Gairome Clay cake at constant pressure filtration can be represented as the sum of the term α_{app}, which includes the variables p and s only, and the correction term α_{corr}, which includes the variables p, s and v. The term α_{app} in the empirical equation of α_{av} indicates the influence of the degree of particle flocculation, the latter depending on the slurry concentrations; while the term α_{corr} in the expression of α_{av} shows the occurrence of cake deflocculation due to the filtrate flow (in other words, the existence of a kind of scouring effect). Studies on the aging of slurries showed that in the empirical correlation $\alpha_{av}=\alpha_0 p^n$ for the average specific filtration resistance, the α_0-value decreased continuously with the elapsed time and the n-value remained practically unchanged.[17]

2. Internal Flow Mechanism in Filter Cake

2. 1. Introduction

Development of filtration theory in recent years has been based upon differential equations involving local flow resistances and variable flow rates. The local filtration resistances have been related to experimental values of compressive pressure by means of the compression-permeability cell as designed by Carman[11] and Ruth.[12] Recent work by Tiller and co-workers[13,34] has led to a better understanding of the internal flow mechanisms. Tiller and Cooper[34] developed a differential equation involving a variable fluid flow rate q. However, they failed to recognize that the movement of the solids was such that the solid velocity could not always be assumed to have a value of zero. This chapter demonstrates how the basic flow equation can be modified to take into account the average liquid velocity relative to the average solid velocity.[14,15]

In Fig. 2. 1, a schematic diagram of a cake is shown. As the cake is compressed, the porosity decreases with time at a given distance, x, from the medium. Decrease in porosity is caused by solid flowing into the voids as the cake compresses. The compressive, squeezing action causes the flow rate of the liquid to

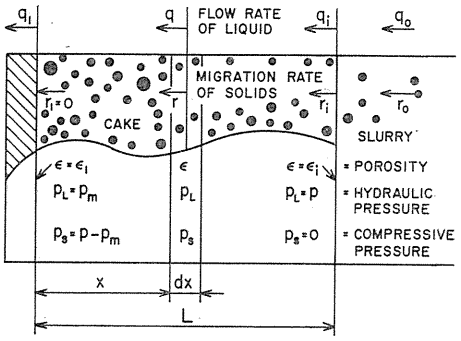

Fig. 2. 1. Schematic diagram of cake.

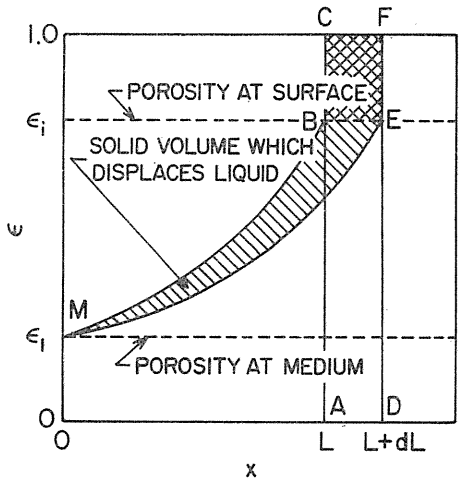

Fig. 2. 2. Porosity vs. distance.

increase as the medium is approached.[13, 34, 35]

In Fig. 2. 2, plots of the porosity ε vs. x are shown in relation to cake thickness L at time θ and thickness $(L+dL)$ at time $(\theta+d\theta)$. The liquid volume squeezed out from the cake during time $d\theta$ is represented by the area MBE, the liquid volume added to the cake by ABED, and the net solid volume is MBCFE. The liquid volume squeezed out of the cake exactly equals the displaced liquid.

Variable flow rates of liquid and solid are of importance in short filtrations involving concentrated slurries as often practiced in continuous, vacuum filters and filter presses. Ordinary filtration equations as used by many investigators[1~3,11,36] can be in error if the slurry is highly concentrated. Errors ranging from 5 to 25% may be encountered if the velocity variations are neglected.

The percentage of voids in filter cakes varies widely. In some cases a cake will contain less than 5% solids by volume; while in other cases, it may run as high as 70% solids. In general for filtration, the slurry must contain less solids than the cake. In fact, the slurry will have a smaller percentage of solids than the surface of the cake where the percentage of solids $(1/m_i)$ is a minimum. Thus the slurry concentration s must be less than $1/m_i$, if the slurry is not, in fact, a cake. A concentrated slurry is one in which s approaches $1/m_i$. It is not possible to define a precise limit for concentrated slurries because of the differences in behavior of different materials.

2. 2. Basic differential equation of filtration

The basic differential equation for filtration has generally been presented in the form.[13]

$$\frac{dp_s}{dw}=\frac{1}{\rho_s(1-\varepsilon)}\cdot\frac{dp_s}{dx}=-\mu\alpha q \tag{2.1}$$

where ρ_s is the true density of solids, p_s the solids compressive pressure, w the mass of cake solids per unit area, α the local specific filtration resistance and q

the apparent flow rate of liquid at a distance x from the medium as shown in Fig. 2. 1. Equation (2. 1) rests upon the assumption that the liquid moves past stationary solid particles. The solids move toward the septum as the cake is compressed during filtration, and it is false to assume that the solid velocity is zero. As a practical matter the velocity of the solids is important for highly concentrated slurries. Equation (2. 1) must be modified where the velocity of the solids is comparable to the velocity of the liquid. A concentrated slurry is roughly defined as one in which the solid content in the slurry contains about 50 to 75% of the solid concentration at the cake surface ($m_i s$ is greater than 0. 5).

It should be recognized that the internal flow rates of liquid, q and solids, r, are not constant due to the continuous compression of the cake.

If ε is the porosity at x, the true average velocity of the liquid is represented by q/ε and the true average velocity of the solids is given by $r/(1-\varepsilon)$. Therefore the true average relative velocity, U, of liquid to solids is represented by

$$U=\frac{q}{\varepsilon}-\frac{r}{1-\varepsilon} \tag{2. 2}$$

Multiplying Eq. (2. 2) by the local porosity, ε, yields the apparent relative flow rate, u, of liquid to solids based upon unit cross-sectional area

$$u=\varepsilon U=q-\frac{\varepsilon}{1-\varepsilon}r=q-er \tag{2. 3}$$

where e is the local void ratio. Replacing the flow rate of the liquid by the flow rate relative to the solids in Eq. (2. 1) leads to

$$\frac{dp_s}{dw}=\frac{1}{\rho_s(1-\varepsilon)}\cdot\frac{dp_s}{dx}=-\mu\alpha(q-er) \tag{2. 4}$$

when flow takes place through a fixed, compressible bed in which the solids are not moving, r is zero and q is constant (although the average liquid velocity q/ε may vary).

2. 3. Differential equations for q and r variation

In order to prove that q/q_1 is a function of x/L, a basic equation relating flow rate to distance will be derived. The void volume per unit cross-sectional area in a differential section of cake equals εdx, and the total void volume is given by

$$\frac{\text{void volume}}{\text{unit area}}=\varepsilon_{av}L=\int_0^L\varepsilon dx \tag{2. 5}$$

where ε_{av} is the average porosity of entire cake. If the upper limit in Eq. (2. 5) is replaced by x, the integral represents the void volume per unit area contained in distance x. Since the porosity is decreasing throughout the cake contained in distance 0 to x, the rate of flow into this portion of the cake q minus the rate of flow out q_1 at the medium (see Fig. 2. 1) must equal the rate of gain of liquid. Mathematically, a material balance gives

$$q-q_1=\frac{\partial}{\partial\theta}\int_0^x\varepsilon dx=\int_0^x\frac{\partial\varepsilon}{\partial\theta}dx \tag{2. 6}$$

where it is assumed that ε is a function which can be differentiated under the integral sign. If Eq. (2.6) is differentiated with respect to x, there results

$$\frac{\partial q}{\partial x}=\frac{\partial \varepsilon}{\partial \theta} \tag{2.7}$$

which was previously developed[34] with an altered sign. This equation was originally derived by Terzaghi[37] in 1923 and is basic to rate-of-consolidation theory in soil mechanics.

The total mass of dry solids per unit area between the septum ($x=0$) and a distance x is given by

$$w=\rho_s\int_0^x(1-\varepsilon)dx \tag{2.8}$$

As the average porosity in the distance zero to x decreases, solids must flow past the point x to replace the displaced liquid. A material balance over the cake from zero to x yields

$$\rho_s r=\frac{\partial w}{\partial \theta}=-\rho_s\int_0^x\frac{\partial \varepsilon}{\partial \theta}dx \tag{2.9}$$

provided there is no solids loss at the septum. The value of r gives the net flow of solids into the given volume. If there is loss of solid through the septum (cloudy filtrate), then Eq. (2.9) would not be valid. Differentiating Eq. (2.9) with respect to x gives

$$\frac{\partial r}{\partial x}=-\frac{\partial \varepsilon}{\partial \theta} \tag{2.10}$$

Combining Eq. (2.7) with Eq. (2.10) yields

$$dq+dr=0 \tag{2.11}$$

which could be developed directly by considering the displacement of liquid by the moving solids. Integration of Eq. (2.11) yields $q+r=$constant; and evaluation of the constant at $x=0$ where $r=0$ and $q=q_1$ produces

$$q+r=q_1 \tag{2.12}$$

Equations (2.11) and (2.12) clearly indicate that variations in q are accompanied by corresponding variations in r.

It is necessary to have formulae for the rate of flow q_i of the liquid and r_i of the solids at the interface of the cake and slurry. Material balances over a differential increase in thickness dL of the cake yield equations leading to values of q_i and r_i. Tiller and Cooper[34] derived an incorrect expression for q_i/q_1 which was later corrected.

For constant pressure filtration with negligible medium resistance in which the average porosity remains constant ($dm/d\theta=0$),[13, 34] it has been shown that the flow rate q_1 at the medium is given by

$$q_1=\frac{dv}{d\theta}=\frac{1-ms}{\rho s}\cdot\frac{dw_0}{d\theta} \tag{2.13}$$

where w_0 is the mass of cake solids per unit area. At the cake surface where fresh solids are deposited, the apparent flow rate q_0 of liquid and r_0 of solids approaching the cake surface may be presented as:

$$q_0=\frac{1-s}{\rho s}\cdot\frac{dw_0}{d\theta} \tag{2.14}$$

$$r_0=\frac{1}{\rho s}\cdot\frac{dw_0}{d\theta} \tag{2.15}$$

It should be noted that both q_0 and r_0 are velocities with reference to any fixed cooordinate or to the medium. Since q_0 and r_0 refer to conditions approaching the cake surface, the sum of q_0 and r_0 does not equal q_1 as indicated by Eq. (2.12). If ε_i denotes the porosity in an infinitesimal surface layer of cake dL deposited in time $d\theta$, the solid volume which remains in the surface layer equals $(1-\varepsilon_i)dL$. One then gets the apparent rate of flow of solids r_i at the cake surface as

$$r_i=r_0-(1-\varepsilon_i)\frac{dL}{d\theta} \tag{2.16}$$

Since $w_0=\rho_s(1-\varepsilon_{av})L$ and ε_{av} is assumed constant, it is possible to eliminate L in Eq. (2.16) and combine with Eq. (2.15) to give

$$r_i=\frac{1}{\rho_s}\left(\frac{\varepsilon_i-\varepsilon_{av}}{1-\varepsilon_{av}}\right)\frac{dw_0}{d\theta} \tag{2.17}$$

Dividing Eq. (2.17) by Eq. (2.13) yields

$$\frac{r_i}{q_1}=\frac{\rho s(\varepsilon_i-\varepsilon_{av})}{\rho_s(1-\varepsilon_{av})(1-ms)}=\frac{(\varepsilon_i-\varepsilon_{av})(m-1)}{\varepsilon_{av}(1-ms)}s$$

$$=\frac{\rho s(\varepsilon_i-\varepsilon_{av})}{\rho_s(1-\varepsilon_{av})-s\{\rho_s(1-\varepsilon_{av})+\rho\varepsilon_{av}\}} \tag{2.18}$$

If the cake is uniform $\varepsilon_i=\varepsilon_{av}$ or $s=0$, then $r_i/q_1=0$. Since the sum of q_i and r_i equals q_1 as indicated by Eq. (2.12), q_i/q_1 can be written as

$$\frac{q_i}{q_1}=1-\frac{(\varepsilon_i-\varepsilon_{av})(m-1)}{\varepsilon_{av}(1-ms)}s$$

$$=1-\frac{\rho s(\varepsilon_i-\varepsilon_{av})}{\rho_s(1-\varepsilon_{av})-s\{\rho_s(1-\varepsilon_{av})+\rho\varepsilon_{av}\}} \tag{2.19}$$

Tiller and Shirato[13] showed that it was possible to assume $\varepsilon=f(x/L)$ for constant pressure filtration with negligible medium resistance. Cake thickness L is a function of θ. Differentiating $\varepsilon=f(x/L)$ with respect to time yields

$$\frac{\partial\varepsilon}{\partial\theta}=\frac{d\varepsilon}{d(x/L)}\cdot\frac{d(x/L)}{d\theta}=-\frac{x}{L^2}\cdot\frac{d\varepsilon}{d(x/L)}\cdot\frac{dL}{d\theta} \tag{2.20}$$

Substituting Eq. (2.20) into Eq. (2.9) and changing the limits from $(0, x)$ to $(\varepsilon_1,$

ε) gives

$$r=\frac{dL}{d\theta}\int_{\varepsilon_1}^{\varepsilon}\left(\frac{x}{L}\right)d\varepsilon \tag{2.21}$$

The value of r_i is obtained when $\varepsilon=\varepsilon_i$. Solving for r/r_i gives

$$\frac{r}{r_i}=\frac{\int_{\varepsilon_1}^{\varepsilon}(x/L)\,d\varepsilon}{\int_{\varepsilon_1}^{\varepsilon_i}(x/L)\,d\varepsilon}=\frac{(\varepsilon-\varepsilon_{av\cdot x})}{(\varepsilon_i-\varepsilon_{av})}\cdot\frac{x}{L} \tag{2.22}$$

where $\varepsilon_{av\cdot x}$ is the average value of ε between zero and x. When $x/L=1$, $\varepsilon=\varepsilon_i$ and $r/r_i=1$; and when $x/L=0$, $\varepsilon=\varepsilon_1$ and $r/r_i=0$. Multiplying Eq. (2.22) by Eq. (2.18) yields

$$\frac{r}{q_1}=\frac{(m-1)s}{\varepsilon_{av}(1-ms)}(\varepsilon-\varepsilon_{av\cdot x})\frac{x}{L} \tag{2.23}$$

Substitution of Eq. (2.23) into Eq. (2.12) yields

$$\frac{q}{q_1}=1-\frac{(m-1)s}{\varepsilon_{av}(1-ms)}(\varepsilon-\varepsilon_{av\cdot x})\frac{x}{L} \tag{2.24}$$

Substitution for m in terms of porosity gives

$$\frac{q}{q_1}=1-\frac{\rho(\varepsilon-\varepsilon_{av\cdot x})s(x/L)}{\rho_s(1-s)(1-\varepsilon_{av})-\rho s\varepsilon_{av}} \tag{2.25}$$

The value of ε_{av} depends chiefly on the applied filtration pressure when the medium resistance is negligible. Therefore q/q_1 is a function of x/L alone at constant s and p.

The apparent relative velocity of the liquid with respect to the solids divided by q_1 is given by

$$\frac{q-er}{q_1}=\frac{q(1+e)-eq_1}{q_1} \tag{2.26}$$

At the medium where $r=0$, the expression in Eq. (2.26) is unity; and at the surface of the cake equals

$$\frac{q_i-e_ir_i}{q_1}=\frac{1-m_is}{1-ms} \tag{2.27}$$

where e_i is the void ratio in an infinitesimal surface layer.

2. 4. Variation of p_L/p and definition of average filtration resistance

Integrating the basic differential equation [Eq. (2.4)] through cake thickness x and the total thickness L and combining the results yields

$$\frac{p-p_s}{p}=\frac{p_L}{p}=\frac{\int_0^{x/L}\{\left(\frac{q}{q_1}\right)(1+e)-e\}\alpha(1-\varepsilon)\,d(x/L)}{\int_0^1\{\left(\frac{q}{q_1}\right)(1+e)-e\}\alpha(1-\varepsilon)\,d(x/L)} \tag{2.28}$$

where p_L is the local hydraulic pressure. A similar derivation in which r was neglected can be found in reference 19. In deriving Eq. (2.28) the filter medium resistance was neglected. The hydraulic pressure variation p_L/p vs. x/L can be obtained by utilizing Eq. (2.28) in connection with compression-permeability experiments.

A new definition of average filtration resistance results when Eq. (2.4) is utilized instead of Eq. (2.1). The average filtration resistance α_{av} is generally given by

$$q_1=\frac{dv}{d\theta}=\frac{p-p_m}{\mu\alpha_{av}w_0}=\frac{p}{\mu(\alpha_{av}w_0+R_m)} \tag{2.29}$$

where p_m is the pressure loss across the filter medium, and is related to the filter medium resistance R_m by $p_m=\mu q_1 R_m$. Employing the first and last terms in Eq. (2.4) and integrating across the entire cake yields

$$\int_0^{w_0}(q-er)\,dw=\frac{1}{\mu}\int_{p_m}^{p}\frac{dp_L}{\alpha}=\frac{1}{\mu}\int_0^{p-p_m}\frac{dp_s}{\alpha} \tag{2.30}$$

The medium resistance is not neglected in Eq. (2.30), and it is assumed that $dp_L=-dp_s$ and $p_L+p_s=p$. The first term in Eq. (2.30) can be multiplied and divided by q_1w_0 to give

$$\int_0^{w_0}(q-er)\,dw=q_1w_0\int_0^1\left(\frac{q}{q_1}-e\frac{r}{q_1}\right)d\left(\frac{w}{w_0}\right) \tag{2.31}$$

Solving for α_{av} in Eq. (2.29) and substituting q_1w_0 from Eq. (2.31) leads to

$$\alpha_{av}=\frac{p-p_m}{\mu q_1w_0}=\int_0^1\left(\frac{q}{q_1}-e\frac{r}{q_1}\right)d\left(\frac{w}{w_0}\right)\cdot\frac{p-p_m}{\int_0^{p-p_m}\frac{dp_s}{\alpha}} \tag{2.32}$$

Equation (2.32) may be written as

$$\alpha_{av}=J_s\frac{p-p_m}{\int_0^{p-p_m}\frac{dp_s}{\alpha}}=J_s\alpha_R \tag{2.33}$$

where α_R is the conventional filtration resistance defined by Carman[11] and Ruth[12] and J_s the correction factor for α_R. For computational purposes J_s can be placed in the form

$$J_s=\int_0^1\left\{1-\frac{(\varepsilon-\varepsilon_{av.x})(m-1)}{(1-\varepsilon)\varepsilon_{av}(1-ms)}s\left(\frac{x}{L}\right)\right\}d\left(\frac{w}{w_0}\right) \tag{2.34}$$

As previously reported by Tiller and Shirato[13], α_R is theoretically the average specific resistance of a compressible bed with the slurry concentration equal to zero. If s were actually zero, there would be no additional solids deposited. In practice, α_R is a good approximation of the average filtration resistance when the slurry is dilute. While too little information is available to generalize, it is probable that the effect of the solid movement can be neglected when the ratio of the fraction of solids in the slurry to the fraction in the surface layer of the cake is less than 0.5.

2. 5. Measurement of hydraulic pressure variation

The direct determination of porosities at different positions in a cake would be time consuming, tedious, and probably inaccurate. An indirect method, consequently, was employed in which the liquid pressure drop was determined as a function of the distance through the solid.[8] With the hydraulic pressure p_L known, the cake compressive pressure p_s can be calculated by using equation $p_s=p-p_L$. Knowing p_s, one can estimate the porosity distribution from compression-cell measurements.

In Fig. 2. 3 the experimental apparatus for determining the liquid pressure distribution is pictured. On the left is the arrangement of probes as they are placed in the cake. Placing them parallel rather than perpendicular to the flow results in minimum disturbance of the filter bed. In actual operation, it was essential to avoid completely vibration of the probes submerged in slurry to prevent channels from developing along the probes with resulting erratic pressure readings. The upper parts of the probes formed a part of the air-sealed manometers shown on the right in Fig. 2. 3. These manometers consisted of seven glass capillaries, 0. 35 mm I. D., 3. 0mm O. D., and approximately 150mm long. One end of each capillary was sealed after a column of mercury, approximately 10mm in length, had been introduced in the other end. Each capillary was connected to one end of a brass tube 2. 5mm I. D., by means of a special fitting consisting of four parts, namely the body of the fitting, a rubber gasket, a gland to retain the gasket, and a cap nut to retain the gland. The other ends of these brass tubes were affixed so as to form a cluster, each tube being approximately 2 to 3mm consecutively shorter than the longest tube. Thus, fairly accurate measurements of the hydraulic pressures at different positions within the filter cake were ensured. The inside diameter of capillaries was limited and controlled by the behavior of the mercury within the tube and was the smallest diameter that would permit the mercury to move uniformly. With a very long hypodermic needle and syringe, the brass tubes were completely filled with water to reduce to a minimum the amount of slurry that could enter the tubes when the filtration pressure was applied. The air in the sealed manometers of Fig. 2. 3 was compressed as the mercury moved upward, the position of the mercury column being calibrated against known pressures. The tubes had to be cleaned frequently, and calibrations were repeated each time the manometers were changed. In Fig. 2. 4 the types of data which were obtained are illustrated for a ignition-plug slurry having a mass fraction of solid equal to 0. 367 and filtered at a constant pressure of 496kPa. As long as a probe remained outside of the cake, the pressure was constant and equal to the applied filtration pressure. As soon as the cake increased in thickness sufficiently to envelop a probe, the pressure began to fall. The

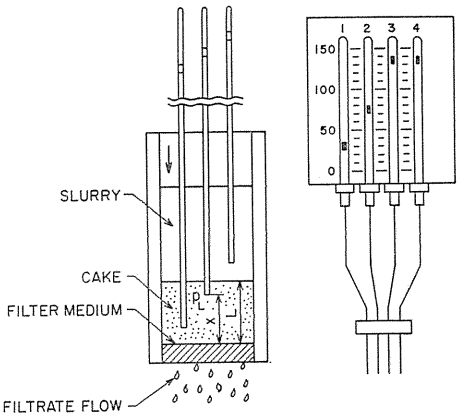

Fig. 2. 3. Schematic diagram of air-sealed manometers.

thickness of the cake could be determined accurately as a function of time or volume filtered by observing the time at which the pressure on a given probe began to fall.

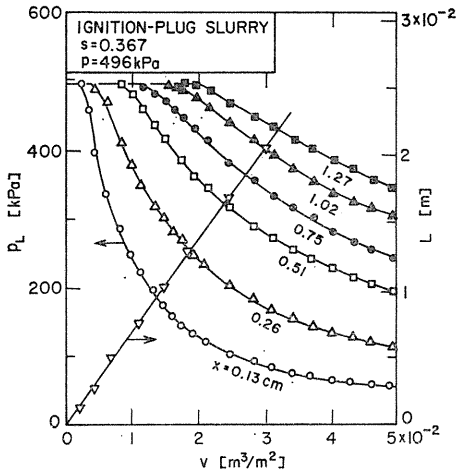

Fig. 2. 4. Variations of hydraulic pressure and cake thickness with filtrate volume.

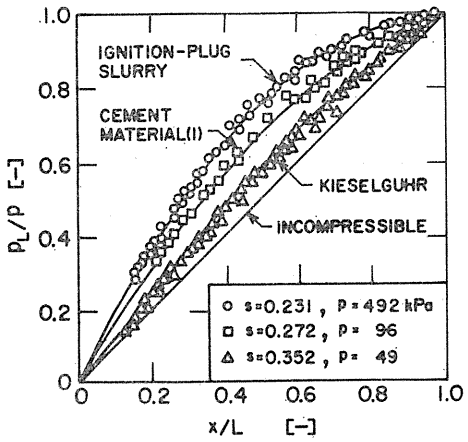

Fig. 2. 5. Hydraulic pressure distributions in cake.

Based upon experiments similar to the one illustrated in Fig. 2. 4, plots of p_L/p vs. x/L were prepared as shown in Fig. 2. 5. It is apparent that time does not appreciably affect the relationship. Previously it was demonstrated with theoretical calculations (Fig. 6 of reference 34) that ε was a function of x/L alone and not θ for a dilute slurry of kaolin after 1 min of filtration. In the first few seconds calculated values for the filtration of kaolin indicated that porosity was a function of time as well as the normalized distance x/L. However a limiting curve of ε as a function of x/L was rapidly approached. When the average experimental filtration resistance becomes constant and the volume vs. time discharge curve is parabolic in a constant pressure filtration, it would be expected that ε would have reached its limiting relation as a unique function of x/L. In short filtrations with thick slurries, where α_{av} is expected to vary with time, the assumption of a unique relation between ε and x/L would not be expected to be valid. In addition to the previous evidence empirical expressions relating ε to the normalized distance x/L were developed.[38] Consequently it is felt that under a wide variety of conditions it may be assumed that ε depends only on x/L.

Since the solid is distributed nonuniformly throughout the cake, it is necessary to show that w/w_0 is a unique function of x/L. The differential dw can be written as

$$dw=\rho_s(1-\varepsilon)dx \tag{2.35}$$

and the total mass of cake w_0 is given by

$$w_0=\rho_s(1-\varepsilon_{av})L \tag{2.36}$$

Dividing Eq. (2.35) by Eq. (2.36) one gets an equation in which the normalized variables can be presented as

$$\int_0^{w/w_0} d\left(\frac{w}{w_0}\right)=\frac{w}{w_0}=\int_0^{x/L}\frac{1-\varepsilon}{1-\varepsilon_{av}}d(x/L) \tag{2.37}$$

Since ε is assumed to be a function of x/L and ε_{av} is constant, w/w_0 is a function of x/L alone.

2. 6. Graphical method for solving constant pressure filtration

The following graphical method is most convenient to evaluate the constant pressure filtration characteristics using the data obtained in a compression-permeability cell.

Rearranging Eq. (2.4), and integrating it through cake thickness x and L, and combining their results leads to

$$\frac{\int_{p_s}^{p}\frac{dp_s}{(1-\varepsilon)\alpha}}{\int_0^{p}\frac{dp_s}{(1-\varepsilon)\alpha}}=\frac{\int_0^{x/L}\left\{\left(\frac{q}{q_1}\right)(1+e)-e\right\}d\left(\frac{x}{L}\right)}{\int_0^{1}\left\{\left(\frac{q}{q_1}\right)(1+e)-e\right\}d\left(\frac{x}{L}\right)} \tag{2.38}$$

As a first approximation, the flow rate q is assumed constant throughout the cake. Then the right hand side of Eq. (2.38) becomes simply x/L. The integration of the left hand side of Eq. (2.38) can be evaluated at any given p_s using data from compression-permeability experiments. Assuming q/q_1 equals unity, the cake compressive pressure distribution p_s/p vs. x/L can be calculated. Knowing the p_s-distribution, the ε-distribution can be obtained using the compression-permeability data. Knowing the ε vs. x/L curve, all terms in the right hand side of Eq. (2.24) are evaluated and the flow rate ratio q/q_1 throughout the cake can be calculated as a unique function of normalized distance x/L.

As a second approximation, the q-distribution thus obtained is assumed. These successive assumptions are continued graphically twice or three times until the maximum deviation in the q/q_1 values of the assumption and the result are less than $\pm 0.5\%$.

In Fig. 2. 6 calculations thus obtained illustrate the variations of q/q_1, r/q_1 and er/q_1 with w/w_0. Figure 2. 6a corresponds to the case in which a slurry has a concentration less than its maximum possible value of $1/m_i$. The value m_i is the ratio of the mass of wet cake to the mass of dry cake in an infinitesimal surface layer. The reciprocal of m_i is simply the fraction of dry solids in the surface layer. When $s=1/m_i$, the slurry reaches a solid state, and it is assumed that lower values of s will normally be encountered. Figure 2. 6b corresponds to the case in which $s=1/m_i$.

When $s=1/m_i$, Eq. (2.19) yields a value of $q_i/q_1=\varepsilon_i$, and $r_i/q_1=1-\varepsilon_i$. The relative velocity $(q_i-e_ir_i)$ at the cake surface is equal to zero. Therefore at the limiting condition for $s=1/m_i$, the liquid and solid are moving with same velocities at the cake surface.

The difference between q/q_1 and er/q_1 represents the average relative velocity. The hatched area equals the value of J_s as defined by Eqs. (2.32)$\sim$(2.34). The

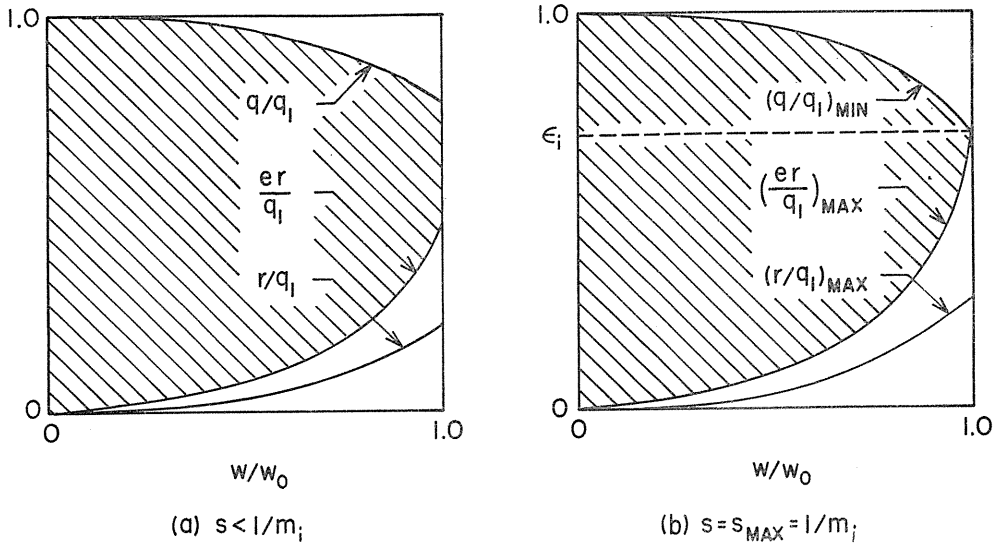

Fig. 2. 6. Variations of q/q_1, r/q_1 and er/q_1 with w/w_0.

value of J_s is at its minimum in the case illustrated in Fig. 2. 6b, and J_s becomes unity when $s=0$.

Calculations of rigorous internal flow variation require accurate data for filtration resistance as obtained from a compression-permeability cell in the form of α and ε as a function of the applied compressive pressure p_s. Using porosity-pressure data obtained from a compression-permeability cell and hydraulic pressure variation data from actual cakes with tubes connected to air-sealed capillary manometers, values of q/q_1, r/q_1 and er/q_1 were calculated for various slurry concentrations for ignition (spark) plug (alumina and clay) and cement material in Figs. 2. 7 and 2. 8. The area between the q/q_1 and er/q_1 curves gives the value of J_s.

It is apparent from Eq. (2. 34) that J_s depends upon filtration pressure and slurry concentration. While the pressure has relatively little effect, the value of J_s may change markedly for concentrated slurries of moderately compressible materials as illustrated in Figs. 2. 9 and 2. 10. For ignition-plug (alumina and clay) slurry filtered at 490kPa, the value of J_s is about 0. 835 which is much smaller than the value reported on the basis of zero solid velocity.[13]

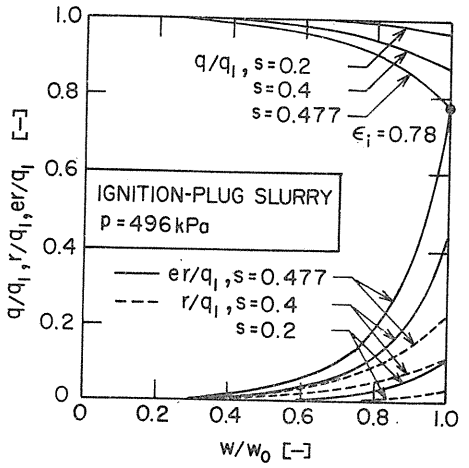

Fig. 2. 7. Variations of q/q_1, r/q_1 and er/q_1 with w/w_0 for ignition-plug slurry.

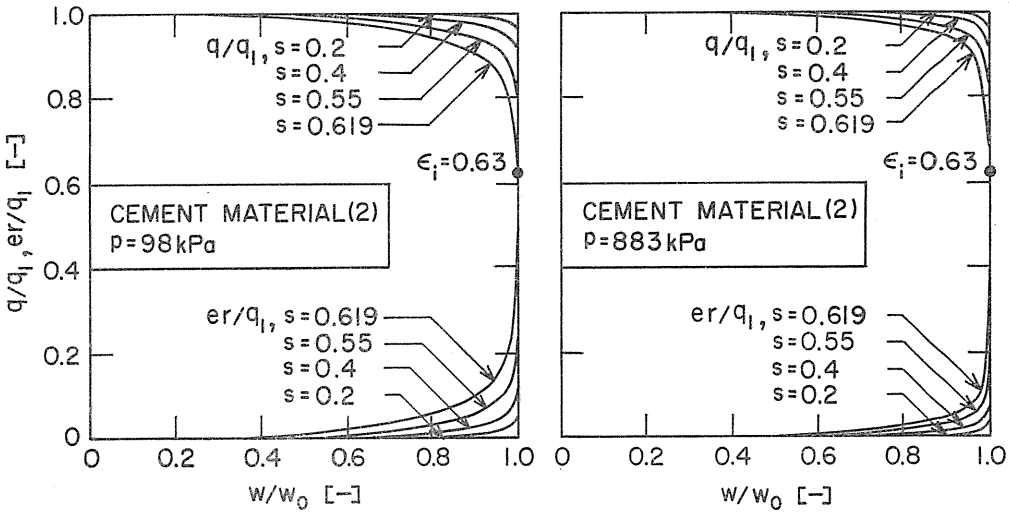

Fig. 2. 8. Variations of q/q_1, r/q_1 and er/q_1 with w/w_0 for cement material (2) slurry.

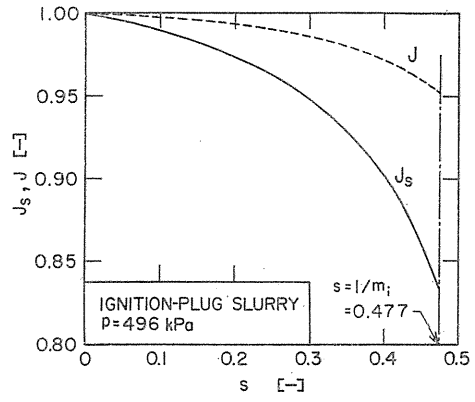

Fig. 2. 9. Effect of s on J_s and J for ignition-plug slurry.

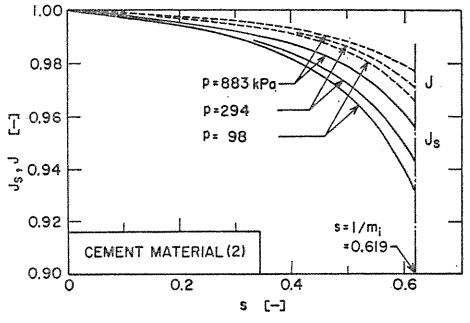

Fig. 2. 10. Effect of s on J_s and J for cement material (2) slurry.

3. Compression-Permeability Tests

3. 1. Frictional drag on particles

When suspended solids are deposited during cake filtration, liquid flows through the interstices of the compressible bed in the direction of decreasing hydraulic pressure. The solids are retained by a screen, cloth, porous metal, or other structure known as the septum or filter medium. The solids forming the cake are compact and relatively dry at the medium, whereas the surface layer is in a wet

and soupy condition. The porosity is minimum at the point of contact between the cake and medium where $x=0$ and maximum at the surface ($x=L$) where the liquid enters. The drag on each particle is communicated to the next particle; consequently, the net solid compressive pressure increases as the medium is approached, thereby accounting for the decreasing porosity.

Assuming that inertial forces are negligible, the balance of forces acting on the solids and the liquid over the slice dx can be represented by the following equations, respectively.

$$\frac{\partial F_s}{\partial x}dx+A\frac{\partial}{\partial x}\{(1-\varepsilon)p_L\}dx+ARdx=0 \tag{3.1}$$

$$A\frac{\partial}{\partial x}(\varepsilon p_L)-ARdx=0 \tag{3.2}$$

The term F_s represents the accumulated drag on the particles and is communicated through the points of contact. The term R represents the viscous drag per unit volume of solids acting on the solid particles within the slice dx. If the particles are in point rather than area contact, the hydraulic pressure p_L may be assumed to be effective over the entire cross-sectional area A of the cake. Combining Eq. (3.1) with Eq. (3.2) and defining the compressive drag pressure by $p_s=F_s/A$ yields

$$\frac{\partial p_L}{\partial x}+\frac{\partial p_s}{\partial x}=0 \tag{3.3}$$

or on integration

$$p_L+p_s=p \tag{3.4}$$

The drag on the particles is a combination of skin and form drag produced by friction developed at the surface of the particles. The drag is transmitted through the points of particle contact. The cross-sectional area does not equal the surface area of the particles or the contact area. Thus p_s is a fictitious or pseudopressure which is introduced for convenience. The applied pressure p may be a function of time but is independent of distance x. Equations (3.3) and (3.4) simply state that drag pressure increases as the hydraulic pressure decreases.

It is generally assumed that the mechanical pressure in the compression-permeability cell produces the same effects as the cumulative frictional drag of liquid passing through the cake. In a filter cake, the drag is cumulative and the compressive pressure varies throughout the cake. One of the most important postulates of filtration states that the porosity and filtration resistances, determined under a given mechanical loading p_s in a compression-permeability cell, are the same as the porosity and resistance at a point where the cake compressive pressure equals the mechanical loading in the cell.

3. 2. Porosity and flow resistance

It is generally assumed in compressible cake theory that the local porosity and flow resistance are unique functions of the drag pressure. These relations can be determined by using the so-called compression-permeability cell.[2~4, 8, 9, 11, 12]

Whereas p_s is measured directly in the compression-permeability cell, it can be calculated only indirectly in the filter cake by means of Eq. (3.4) with the directly measurable quantities p and p_L.

The apparatus employed consists essentially of a container in which samples can be placed and subjected to vertical loading, as shown in Fig. 3. 1. In the simplest type of testing, the sample is placed between porous plate and kept saturated with water while the load is applied. At the instant the load is added, the stress is applied to both the solid particles and the liquid within the interstices. Since the liquid is free to flow through and around the porous plates, the excess of liquid pressure above atmospheric, referred to as the neutral stress, causes the moisture to leave the voids, resulting in a consolidation of the solids. As the water flows out, the neutral stress drops, the solids finally carrying the applied load. After the entire load comes to be borne by the solids, the equilibrium value of the porosity ε can be determined. The load per unit area is designated as the compressive pressure p_s. The flow rate of water from the sample depends upon the permeability, and the time required to reach equilibrium ranges from several hours to 24h. Then, the liquid is allowed to flow through the compressed cake under relatively small head p. The flow resistance α can be calculated as follows:

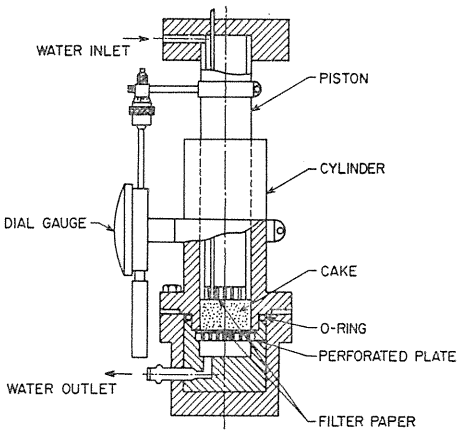

Fig. 3. 1. Schematic diagram of compression-permeability cell.

$$\alpha=\frac{p}{\mu q_1 w_0} \tag{3.5}$$

where q_1 is the permeation rate and w_0 the solids mass of entire cake per unit area.

As a fair approximation of compression-permeability data for many materials, the various functional relations between the porosity, flow resistance and compressive pressure can be used as follows:

$$\left.\begin{aligned}&\varepsilon\fallingdotseq\varepsilon_i, \quad p_s\leqq p_i\fallingdotseq 0\\&\varepsilon\fallingdotseq\varepsilon_0 p_s^{-\lambda}, \quad p_s>p_i\end{aligned}\right\} \tag{3.6}$$

$$e=e_0-C_c\ln p_s \tag{3.7}$$

$$\left.\begin{aligned}&\alpha\fallingdotseq\alpha_i, \quad p_s\leqq p_i\fallingdotseq 0\\&\alpha=\beta_p+\alpha_{op}p_s^{\,n}\fallingdotseq\alpha_{op}p_s^{\,n}, \quad p_s>p_i\end{aligned}\right\} \tag{3.8}$$

It is assumed that the flow resistance and porosity take on constant values, α_i and ε_i, at the same low pressure p_i which is generally in the range of 10kPa. The values of flow resistance and porosity are related by

$$\alpha=\frac{kS_0^2(1-\varepsilon)}{\rho_s\varepsilon^3} \tag{3.9}$$

where k is Kozeny's constant, S_0 the effective specific surface of cake solids.

3. 3. Limitations of compression-permeability cell techniques

Development of the methematical art of filtration in recent years depends upon several assumptions. Among the most important postulates are

1. Ultimate values of porosity are attained instantaneously in accordance with the progress of filtration process. This assumption can be deduced to be valid for filtration in which filtration pressure increases slowly just as usual practical filtration.

2. The local filtration resistance α of a given solid is determined by the local porosity ε, which in turn depends only upon the local cake compressive pressure p_s. This assumption may be invalid when the filtration resistance is affected by the velocity of filtrate flow. It may occur for filtration of slurries of very wide particle-size distribution, and also may be likely to occur when the filtration velocity is extraordinarily high.

3. The porosity and specific filtration resistance determined under a given mechanical loading p_s in a compression-permeability cell is the same as the local porosity and local specific resistance at a point in a filter cake where the cake compressive pressure (computed by $p_s=p-p_L$) is the same as the mechanical loading to the piston of the cell. To measure the porosity in a compression cell, a definite period of time ranging from several hours to longer than twenty hours (about ten hours being common for clay materials) is required to reach an equilibrium porosity. Thus the assumption of item 3 is actually invalid if the filtration characteristics of a slurry may change with the lapse of time. Furthermore, there will be appreciable side friction between the wall of the cell cylinder and the compressed cake.

As the mathematical theory of filtration may largely rest on the assumption of item 3, it is the most important assumption. The results of Grace,[2,3] Kottwitz and Boylan,[7] and Okamura and Shirato[8,9] lent validity to the postulate, and Okamura and Shirato made verification of the postulate by simultaneous determination of porosity[19,20] and hydraulic pressure variations[8] within actual filter cakes. It should be noted that they used the slurry materials of finely ground natural clays of various kinds. The filtration characteristic of finely ground clay slurries may not so suffer the aging effect, whereas the chemical precipitates, diatomacious filter aids produced by flux calcination, Solka-Floc and slurries which contain organic matters including sewage sludge usually suffer the aging effect and it is found that there is an appreciable difference between the compression-permeability data and actual filtration results by experimentation of many workers.

Concerning the effect of side-wall friction on the uniformity of packing of beds in compression-permeability cell, Grace[2,3] mentioned that compression-permeability data showed good reproducibilities if thickness to diameter ratio Z/D of a compressed cake did not exceed 0.5 or 0.6. Actually there is appreciable side friction[5,39] between the wall of the cell and the compressed cake, and all data obtained in compression-permeability cells must be corrected for the frictional effects. Tiller, Haynes and Lu[40] found that more than 20% of applied load on the cake in a 5.1cm diameter cell was consumed as side wall friction in 2.5cm

cakes and 60% in 7.6cm cakes.

Although investigators[2,3,8,9] recognized the existence of wall friction in the compression-permeability cell, correlations were based upon the assumption that friction could be neglected. No general correlation for the wall friction being available in spite of the efforts by Tiller, Haynes and Lu[40] who measured stress distribution in the compression-permeability cell, an approximate expression was developed.[18~20]

In Fig. 3. 2, the horizontal and vertical pressures in a cell are illustrated. In the field of soil mechanics, it is assumed that the horizontal pressure p_h is proportional to the vertical pressure p_v which can be expressed by

$$p_h = k_0 p_v \tag{3.10}$$

where k_0 is the coefficient of earth pressure at rest, and is assumed to be a constant for each material. Little information concerning the values of the coefficient of friction f at the side wall is available. Utilizing the concept of side friction and assuming that the vertical load is uniformly distributed across the cell and that there exists a constant cohesive force C at the wall, a force over a differential height of cake can be written as

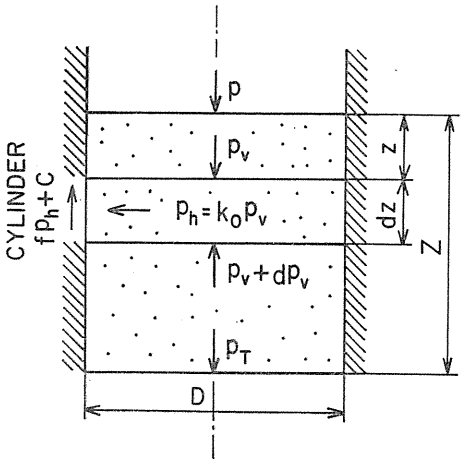

Fig. 3. 2. Schematic diagram of vertical and horizontal pressures in compression-permeability cell.

$$\left(\frac{\pi D^2}{4}\right)\{p_v - (p_v + dp_v)\} = (k_0 f p_v + C)\pi D dz \tag{3.11}$$

where z is the distance from the cake surface. Rearranging and solving Eq. (3.11) for p_v subject to $p_v = p$ at $z = 0$ yields

$$p_v = \frac{1}{k_0 f}\left\{\frac{k_0 f p + C}{\exp(4k_0 f z/D)} - C\right\} \tag{3.12}$$

where p is the applied pressure at the top. Substituting limits $p_v = p_T$ at $z = Z$ leads to

$$p_T = \frac{1}{k_0 f}\left\{\frac{k_0 f p + C}{\exp(4k_0 f Z/D)} - C\right\} \tag{3.13}$$

where p_T is the transmitted value of p_v at the bottom of the cake. The average compressive pressure p_s may be defined by

$$p_s = \frac{1}{Z}\int_0^Z p_v dz \tag{3.14}$$

Substituting Eq. (3.12) into Eq. (3.14) results the following equation.

$$p_s=\frac{p+(C/k_0f)}{4k_0fZ/D}\{1-\exp(-4k_0fZ/D)\}-\frac{C}{k_0f} \tag{3.15}$$

Obviously, with variable stress through compressed cake, all data obtained in the compression-permeability cell would better be correlated with p_s defined by Eq. (3.15) rather than with the applied load p as conventionally reported.

The compression cell used for studying the side wall friction is a modified form of the compression-permeability cell commonly used. Mechanical pressure is applied to the cell piston by weights and transmitted pressure to the bottom of compressed cake is measured by a force transducer, with accompanying wire strain gauges. The transmission mechanism is composed of a brass disk held between two rubber membranes of thickness 0.4mm. The pipe leading to the strain gauge pressure head is completely filled with water and the pressure head performance is calibrated by blank tests. In addition to the side wall friction tests, the normal compression-permeability tests are also conducted.

Compression results are shown in Fig. 3.3, where the ratio of transmitted pressure to applied pressure p_T/p are plotted against final thickness at each constant load. Numerous experiments for measuring p_T and Z at various loads may give the values of k_0f and C on the basis of the minimum root-mean-square deviation of measured values of p_T from those calculated by Eq. (3.13). The values of k_0f and C being known, a porosity-pressure relation as illustrated in Fig. 3.4 may be obtained using Eq. (3.15). It is apparent from Fig. 3.4 that

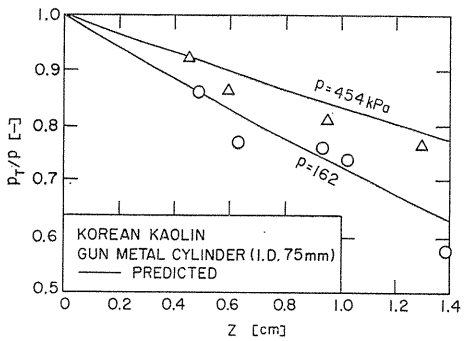

Fig. 3.3. Relation between fraction of transmitted pressure and thickness of compressed cake.

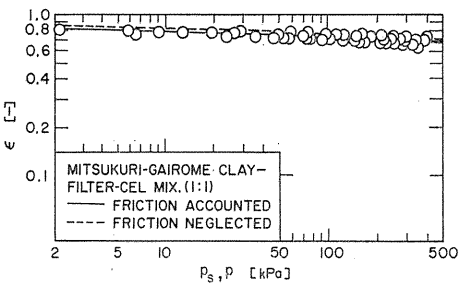

Fig. 3.4. Compression data.

there exists a difference between the conventional plots of ε vs. p_s and the ε vs. p relation corrected for the wall friction.

With variation of compression stress through the compressed cake, it is impossible to assume that the cake in the cell has a uniform resistance. Therefore all data conventionally obtained in permeability cells must also be modified. As a first approximation for representation of permeability test data, the average compressive pressure p_s defined by Eq. (3.15) is utilized instead of the applied load p. It may be seen from Fig. 3.5 that there is an appreciable difference between the relations of α vs. p_s and α vs. p. Since the analysis and the experiments for determining the cell-wall friction are based on one side drainage (upward squeez-

ing), all compression tests for this study are conducted under the condition of one side drainage.

The experimental results attempted in this study are tabulated in Table 3. 1. Side-wall friction and cohesive force of plastic cell cylinders are relatively large, possibly because the inner surface of plastic cylinders may be depressed by solid particles under compression. For more accurate analysis of compressive pressure distribution in a compressed cake which may vary both in the vertical and radial directions, more accurate and elaborate theories and measurements might

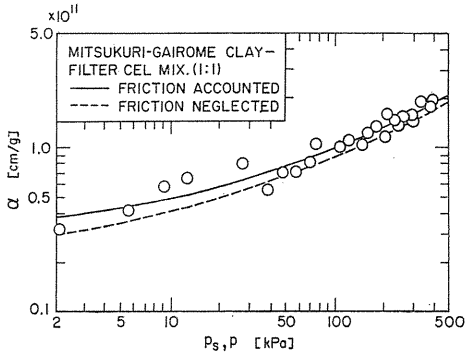

Fig. 3. 5. Permeability data.

Table 3. 1. Values of $k_0 f$ and C.

Material of side wall	$k_0 f$ [−]	C [kPa]
Gun metal	0. 21	54
Plastic	0. 43	69
Brass	0. 56	44
Stainless steel	0. 29	15

be required. However, authors are inclined to use the approximate modification based upon Eq. (3. 15) which is felt to be fairly accurate for the prediction of filtration characteristics.

It is well known[40] that the value of specific resistance increases with prolonged permeation time. In order to minimize the unfavorable effects (possibly filtration effects, consolidation due to permeation, deflocculation, aging, etc.) associated with long permeation times, the permeability tests are conducted only for short times under a reasonable low pressure difference.

Although important to filtration theory, here is considerable difficulty in obtaining accurate values of compression-permeability cell data in the low compressive pressure range. In the low compressive pressure range, the compression-permeability cell method is not adequate because of difficulties related to disturbance of the soft cake; such effects arising in both compression and permeation. In order to determine accurately the compression and permeability characteristics in the low pressure range, an analytical method[41, 42] using batch sedimentation data of a slurry was developed.

When filtration operations are performed under the conditions of rapid pressure increase, sudden change in pressure or rate, and oscillation of applied pressure (as may occur when using a positive displacement pump), the postulate item 1 may become invalid as the basic equivalence of equilibrium porosity conditions in the cell and actual filter cake will not be attained. This fact was realized from filtration experiments conducted under constant rate conditions as shown later in

Chapter 5.

Many workers in this field have compared the results of experimental filtration and compression-permeability cell data. Several workers have failed in obtaining good agreement between the two and enormous errors in prediction have been found. However, it should be noted that the compression-permeability cell techniques rest on several important assumptions listed before. On the basis of an extensive experimental analysis, the present authors have found reasonable, good agreement for clay slurries and significant differences for organic slurries, and others. It is believed that compression-permeability cell techniques are valid when the compression-permeability experiments and the filtration experiments are conducted under consistent conditions with careful consideration being given to the selection of the slurries used in the experimentation. Furthermore, compression-permeability cell techniques will be particularly useful for research oriented studies because they can afford a firmer understanding of the internal mechanism of cake filtration. On the other hand, they may not be well adopted for industrial practice because they are tedious and time-consuming, and suitable slurries applicable for investigation are limited.

3. 4. *Approximate analytical equations for hydraulic pressure distribution*

When the slurry concentration s is so small that the flow rate of filtrate q can be regarded as constant through the entire cake, Eq. (2. 38) simply becomes

$$\frac{\int_{p_s}^{p} \frac{dp_s}{(1-\varepsilon)\alpha}}{\int_{0}^{p} \frac{dp_s}{(1-\varepsilon)\alpha}} = \frac{x}{L} \tag{3. 16}$$

The power relation may be used to approximate the porosity vs. solid compressive pressure data as follows:

$$\left.\begin{aligned} 1-\varepsilon &= 1-\varepsilon_i, \quad p_s \leqq p_i \fallingdotseq 0 \\ 1-\varepsilon &= E' p_s^{\lambda'}, \quad p_s > p_i \end{aligned}\right\} \tag{3. 17}$$

It should be noted that Eq. (3. 17) is incompatible with Eq. (3. 6). From experimental results,[8, 9] it has been known that the value of kS_0^2 in Eq. (3. 9) varies with the porosity ε. In many cases, however, it can be assumed to be constant for approximate calculations.

Neglecting p_i and substituting Eqs. (3. 6), (3. 9) and (3. 17) into Eq. (3. 16) yields

$$\frac{\int_{p_s}^{p} \frac{\varepsilon_0^3 p_s^{-3\lambda}}{kS_0^2 E'^2 p_s^{2\lambda'}} dp_s}{\int_{0}^{p} \frac{\varepsilon_0^3 p_s^{-3\lambda}}{kS_0^2 E'^2 p_s^{2\lambda'}} dp_s} = \frac{x}{L} \tag{3. 18}$$

Calculation of the above expression results in

$$1-\left(\frac{p_s}{p}\right)^{1-2\lambda'-3\lambda} = \frac{x}{L} \tag{3. 19}$$

or

$$\left(1-\frac{p_L}{p}\right)^{1-2\lambda'-3\lambda}=1-\frac{x}{L} \tag{3.20}$$

Equation (3.20) is an approximate analytical equation of the p_L-distribution based upon the validity of a power function relationship between ε and $(1-\varepsilon)$ vs. p_s, under the condition of neglecting the variation of flow rate and kS_0^2 through cake. Permeability experiments are not required in order to calculate the p_L-distribution by Eq. (3.20).

Neglecting p_i and substituting Eqs. (3.8) and (3.17) into Eq. (3.16) yields

$$\frac{\int_{p_s}^{p}\frac{dp_s}{\alpha_{op}E'p_s^{n+\lambda'}}}{\int_{0}^{p}\frac{dp_s}{\alpha_{op}E'p_s^{n+\lambda'}}}=\frac{x}{L} \tag{3.21}$$

and, therefore

$$1-\left(\frac{p_s}{p}\right)^{1-n-\lambda'}=\frac{x}{L} \tag{3.22}$$

or

$$1-\left(\frac{p_L}{p}\right)^{1-n-\lambda'}=1-\frac{x}{L} \tag{3.23}$$

Equation (3.23) is also an approximate analytical equation of the p_L-distribution under the condition of neglecting the variation of flow rate through cake. Equation (3.23) requires the both compression and permeability data, whereas Eq. (3.20) requires only compression data.

4. Porosity Variation in Filter Cake

4. 1. Introduction

In filter cakes the variation of porosity with distance from the cake surface is important from both theoretical and industrial viewpoints. In the development of filtration theory porosity plays a fundamental role in its relation to flow rates, pressure, and other parameters involved in the differential equations of flow through compressible, porous media. Porosity variation determines the average porosity and liquid content of the filter cake in commercial operation.

In 1955 Okamura and Shirato[8] measured the hydraulic pressure variations through filter cakes, initially using air sealed manometers and later strain wire gauges. In 1967 Baird et al.,[43] using nine pairs of metal electrode-pins of 1.27 cm length, measured the variations of electric resistance through a filter cake. Although the resistances were not converted into local porosity values in the cake, the authors deduced that a collapse occurred in the filter cake when filtration had been going on for some time and a critical thickness had been reached. They concluded that the porosity variation was not uniform, as had been conventionally

assumed, and the minimum porosity in a filter cake was not always adjacent to the filter medium. This special type of packing compressibility was formerly called "retarded packing compressibility" (R. P. C.) by K. Rietema.[44]

In this chapter, the local porosity variations in constant pressure filtration cake measured by an electrical method are shown.[19,20] Contrary to the conclusions of Baird et al.,[43] the experimental results show the propriety of the fundamental postulates of filtration theory.[15]

4. 2. Electrical measurements of porosity

In Fig. 4. 1, a compression test cell used is shown. The cell consists essentially of a piston with a porous end and a cylinder, both made of plexiglass which are electrical insulators. At the center of the cell bottom, a wire-strain-gauge pressure transducer is fixed to measure the transmitted pressure p_T. In order to conduct the electrical measurements of porosity in compressed cakes, a pair of platinum electrodes are mounted in the cell cylinder with dimensions of the electrodes being 3 mm diameter and 1 mm thickness. Instead of the pin-type electrodes which protrude into cake as attempted by Baird et al.,[43] disk-type electrodes are employed which are flush with the wall of the cylinder as shown in Fig. 4. 2 to minimize interference with compressed cake. The experiments are carried out using 50wt% Mitsukuri-Gairome Clay-50wt% Filter Cel mixture slurry with a solid concentration of 20wt% in 0. 93wt% solution of salt.

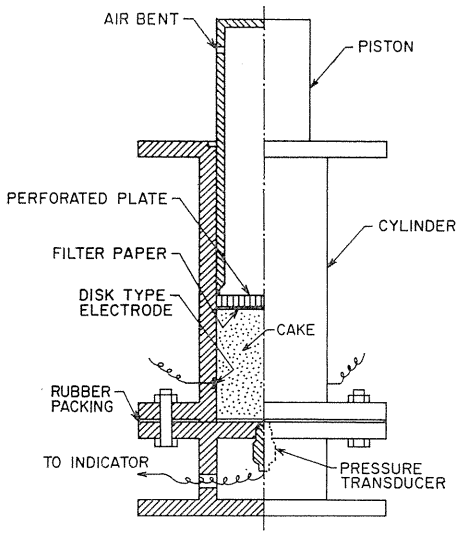

Fig. 4. 1. Schematic diagram of compression cell.

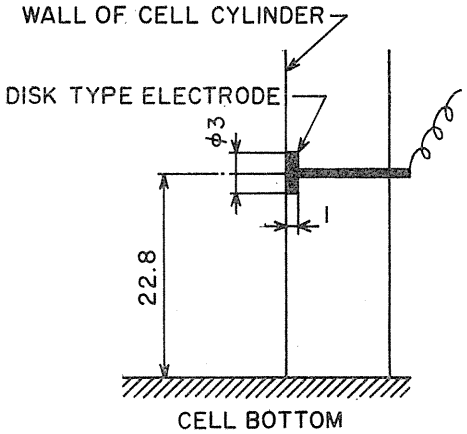

Fig. 4. 2. Schematic diagram of electrode assembly.

In electrical measurements of the porosity of a porous medium, Archie[45] showed empirically that the so-called "formation factor" F defined by

$$F=\frac{\text{Electric resistance of saturated porous medium, } R}{\text{Electric resistance of the saturating fluid at the same temperature, } R_0} \qquad (4.1)$$

could be related to the porosity ε of the medium by a relation of the form

$$\varepsilon = F^{\beta} \tag{4.2}$$

where β is a factor depending on the system concerned. However, Eq. (4.2) may not necessarily be proper for all cases and an attempt should be made to find the best correlation for each case.

First, a saline solution of 0.93wt% NaCl is poured into the cell cylinder and the resistances, R_0, of the liquid at various temperatures are measured, the results being shown in Fig. 4. 3. Then, compression tests of slurry are carried out. The resistance of the compressed cake R, the cake thickness Z and the temperature of liquid are measured when the compression equilibrium is reached, and a further load increment is applied. The formation factor is calculated from the electric resistance of the compressed cake and the curve shown in Fig. 4. 3.

The value of the local solid compressive pressure p_{vE} at the electrodes being known from the following equation

$$p_{vE} = \left(p + \frac{C}{k_0 f}\right)\exp\left\{-\frac{4k_0 f}{D}(Z - z_E)\right\} - \frac{C}{k_0 f} \tag{4.3}$$

the value of the local porosity ε at the depth of electrodes can be evaluated by using the compression test results of ε vs. p_s corrected for the frictional effect. In Eq. (4.3), z_E is the height of the center of the electrode disk measured from the bottom of the cell.

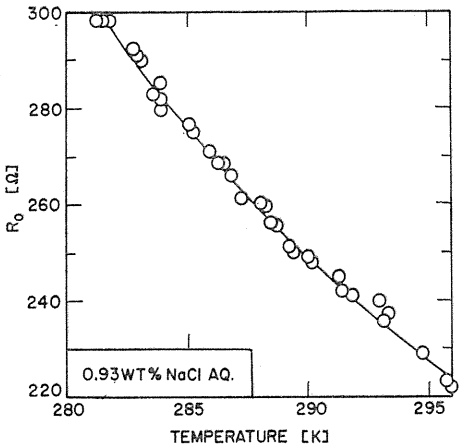

Fig. 4. 3. Effect of temperature on resistance R_0.

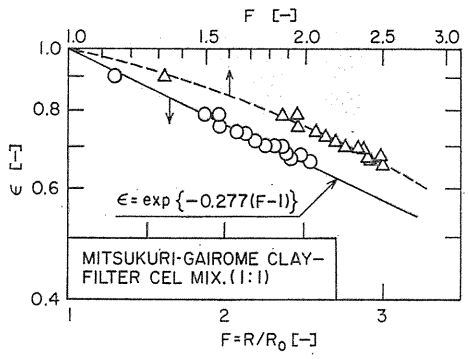

Fig. 4. 4. Relation between porosity and formation factor.

As clearly indicated in Fig. 4. 4 of porosity ε vs. formation factor F, it is apparent that semilogarithmic plots of the following form

$$\varepsilon = \exp\{-0.277(F-1)\} \tag{4.4}$$

are more appropriate rather than logarithmic plots of the form of Eq. (4.2).

4. 3. Experimental equipment and procedure

To conduct constant pressure filtration experiments, the filter shown in Fig. 4. 5 is used to give the distributions of electric resistance R and hydraulic pressure p_L in cake. The filter consists essentially of a plexiglass cylinder of inside diameter 200mm, a stainless-steel top disk and a bottom plexiglass disk which supports a perforated plexiglass plate with a sheet of filter paper on it. The top disk is fitted with an inlet and a returning conduit of slurry, six probes for measurement of hydraulic pressure p_L and two vertical sealed plexiglass pipes of outside diameter 20. 2mm having six pairs of platinum disk-type electrodes. Each pair of electrodes faces each other at a distance of 6 cm. Fitting of the two vertical pipes to the top disk is done carefully so that their bottoms contact the filter paper when the filter equipment is assembled. The electrodes for measuring electric resistance R are arranged at distance of 10. 5, 20. 4, 30. 4, 40. 5, 50. 4 and 60. 5mm and the probes for measuring p_L at distances of 1. 8, 6. 4, 19. 3, 28. 1, 39. 4 and 53. 2mm from the medium. A plan view of the arrangements is shown in Fig. 4. 6.

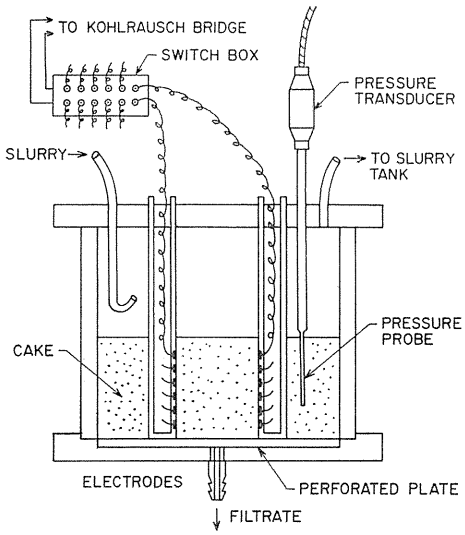

Fig. 4. 5. Schematic diagram of the filter used.

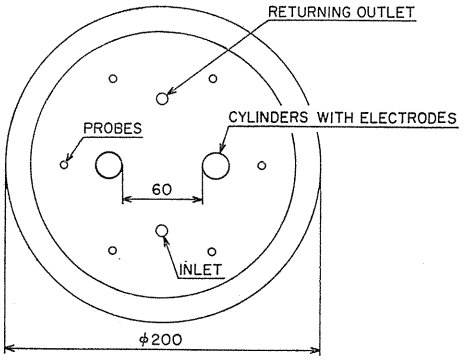

Fig. 4. 6. Plan view of the arrangements of filter.

Filtrate passes through a rotameter and runs into a measuring cylinder.

To avoid sedimentation of solids in the flow line and the filter chamber, a portion of slurry is recirculated by a small centrifugal pump. The rotating blades of the pump are made of rubber so that the effects on the particles in slurry can be minimized. In Fig. 4. 7, the flow lines and wiring diagrams of the measurement devices are shown schematically.

After the filtrate line from the medium to the rotameter is filled with 0. 93% salt solution of the same concentration as that of the filtrate, the filter equipment is assembled and then the filter chamber is filled with slurry with the pump. Constant pressure filtration experiments are carried out by applying compressed

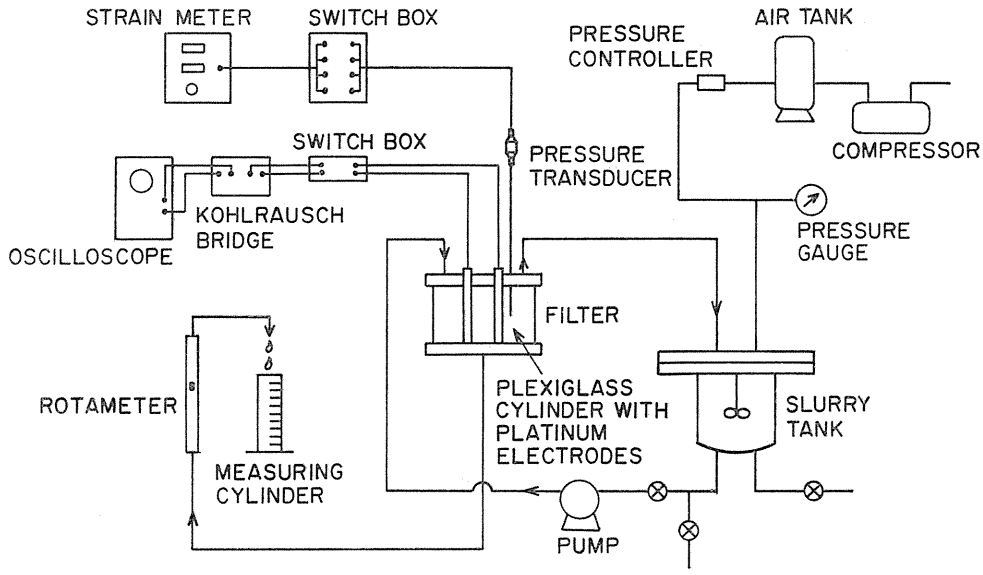

Fig. 4. 7. Flow lines and wiring diagrams of measurement devices.

air pressure. R-distributions are measured by using a Kohlrausch bridge and an oscilloscope, p_L-variations by a pressure transducer and an indicator, and the volume of filtrate and its temperature are obtained at various intervals of filtration time. The slurry used in these experiments is the same as that used in the compression cell test.

4. 4. Experimental results and discussion

Figure 4. 8 illustrates the experimental results of the variations of the formation factor F defined by Eq. (4. 1) during a constant pressure filtration. Figure 4. 8 was prepared from the measured values of R at various depths in the cake and accounting for the pre-determined temperature dependency of R_0 of each pair of electrodes; the latter shown in Fig. 4. 3.

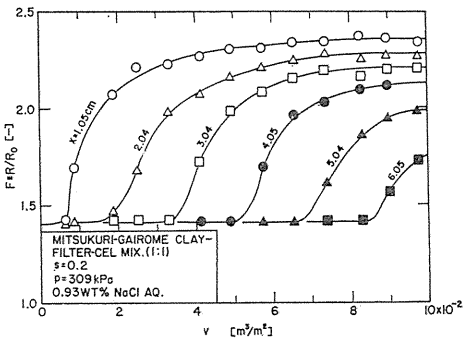

Fig. 4. 8. Variations of formation factor with filtrate volume.

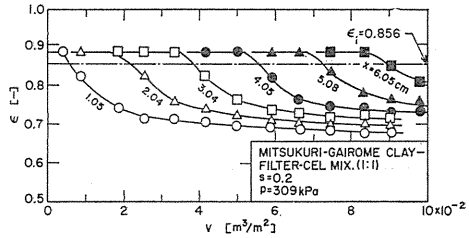

Fig. 4. 9. Variations of porosity with filtrate volume.

By using Eq. (4.4), the formation factors in Fig. 4. 8 can be converted into the porosities as shown in Fig. 4. 9. Figure 4. 9 indicates that the porosity at any point in cake decreases monotonously with the filtration time and approaches a constant value depending on the filtration pressure. In this study, the so-called "retarded packing compressibility" is never observed (see Fig. 4. 9), and the porosity variation is consistent with the so-called "modern filtration theory".

Contrary to the results obtained in this study, Rietema[44] and Baird et al.[43] reported that R. P. C. phenomena were observed, using metal pin-type electrodes which were 1.27cm in length and ran parallel to each other at a horizontal distance of 1.27cm. It might be concluded that abnormal phnomena had occurred, perhaps because the metal pins had supported the cake.

Figure 4. 10 shows the experimental data of porosity versus normalized distance x/L, where cake thickness L is determined from p_L-variations shown in Fig. 4. 11.

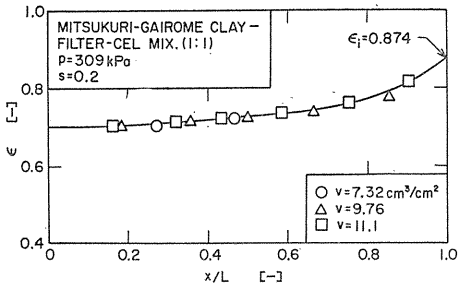

Fig. 4. 10. Relation between local porosity and normalized distance.

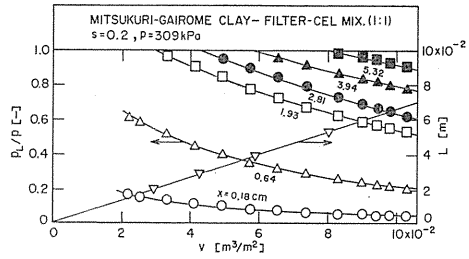

Fig. 4. 11. Variations of hydraulic pressure with filtrate volume.

In Fig. 4. 10, the theoretically determined porosity distribution curve[15] is also shown; the latter utilizing compression-permeability measurements. In modern filtration thery, there is a basic assumption that under constant pressure filtration the local porosity depends upon the normalized distance x/L only when filtration has proceeded for some time. Figure 4. 10 may support the validity of this basic assumption.

Some doubt exists concerning the accuracy of measurements of local porosity by the electrical method as attempted in this chapter. Because of the rather long distance between the electrodes, the flux of electric current may naturally bend towards the direction of smaller resistance in the cake, i. e. of larger porosity as shown in Fig. 4. 12. Therefore, one may obtain a somewhat larger value of porosity than the actual local value and a necessary modification to the observed value of formation factor should be made. It appears that the good agreement shown in Fig. 4. 10 rests on the fact that the cake thickness attempted in this study is

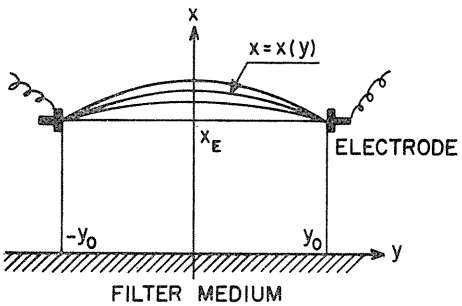

Fig. 4. 12. Schematic diagram of electric current path.

very thick, up to 7 cm.

To improve further the accuracy of measurements of local porosity by the electrical method, the distance between electrodes should be minimized to the extent possible without having serious negative effects. Furthermore, one should make a possible modification for the electric flux path.

On the rough assumption that the electric current may flow mainly along the path of minimum resistance, electric resistance R_0 for filtrate may be written as

$$R_0=\frac{1}{\sigma}\cdot\frac{2y_0}{A_E} \tag{4.5}$$

where y_0 is a half distance between electrodes, A_E the plate area of disk type electrode and σ an empirical constant depending mainly on the electric conductivity of filtrate. The apparent electric resistance of cake, R_A, can be expressed by

$$R_A=\frac{1}{\sigma A_E}\int_{-y_0}^{y_0}\frac{\sqrt{1+\left(\frac{dx}{dy}\right)^2}}{\varepsilon(x)}dy \tag{4.6}$$

for the system in which the porosity changes in accordance with a continuous relation of $\varepsilon\equiv\varepsilon(x)$. The current-path function $x\equiv x(y)$ in Eq. (4.6) means a stationary curve, i. e., the minimum resistance curve for the function expressed by

$$\Phi\{x\}=\int_{-y_0}^{y_0}\frac{\sqrt{1+\left(\frac{dx}{dy}\right)^2}}{\varepsilon(x(y))}dy \tag{4.7}$$

On the other hand, one should obtain the true local value of electric resistance R_T in the cake corresponding to the straight path of current exactly at height x_E of the electrode, i. e.,

$$R_T=\frac{1}{\sigma A_E}\cdot\frac{2y_0}{\varepsilon(x_E)} \tag{4.8}$$

Combination of Eqs. (4.5), (4.6) and (4.8) yields the relation between the true and the apparent value of the formation factors in the form

$$R_T/R_0=(R_A/R_0)\cdot f_E \tag{4.9}$$

or

$$F=F_A f_E \tag{4.10}$$

where f_E is defined by

$$f_E\equiv R_T/R_A\equiv\frac{2y_0}{\varepsilon(x_E)}\int_{-y_0}^{y_0}\frac{\sqrt{1+\left(\frac{dx}{dy}\right)^2}}{\varepsilon(x)}dy \tag{4.11}$$

Therefore, the apparent value of formation factor F_A may be modified by using the correction factor f_E defined by Eq. (4.11).

In most cases, the correction factor f_E seems to be nearly unity and can be accurately determined except for the case where the electrode is extremely close

to a discontinuous layer such as a cake surface. Although the correction factor f_E is assumed to be approximately unity in this study, experimental values of porosity show good agreement with those determined from the so-called modern filtration theory.

5. Constant Rate and Variable Pressure-Variable Rate Filtration

5. 1. Introduction

Filtration operations have been classified into three classes—constant pressure, constant rate, and variable pressure-variable rate filtration—according to the variations of pressure and flow rate with time. In the literature. by far the greatest attention has been focussed on constant pressure filtration which is tractable mathematically.[6, 7, 11, 12, 16, 18] Constant rate and variable pressure-variable rate filtration operations are more often encountered in industry, and, in particular, where a centrifugal pump is used for pumping the slurry into the filter chamber. This may be the most important operation in the process industries. However, relatively little work has been reported in connection with constant rate and variable pressure-variable rate filtration.[5, 39] In this chapter methods of solving constant rate and variable pressure-variable rate filtration problems are presented on the basis of modern cake filtration theory.[18, 21]

5. 2. Variation of q through the cake

The equation for the flow rate variation through cake can be derived on the basis of the continuity Eq. (2. 7). Integrating Eq. (2. 7), one gets

$$q-q_1=\frac{\partial}{\partial\theta}\int_0^x \varepsilon dx \tag{5. 1}$$

The average porosity $\varepsilon_{av\cdot x}$ for cake lying between the medium and a distance x is defined by

$$\varepsilon_{av\cdot x}=\frac{1}{x}\int_0^x \varepsilon dx=\frac{1}{x/L}\int_0^{x/L} \varepsilon d\left(\frac{x}{L}\right) \tag{5. 2}$$

Substituting the differentiation of Eq. (5. 2) into Eq. (5. 1), one gets

$$q-q_1=-\frac{dL}{d\theta}\cdot\frac{x}{L}(\varepsilon-\varepsilon_{av\cdot x}-E) \tag{5. 3}$$

where

$$E=L\int_0^{x/L}\frac{\partial\varepsilon}{\partial\theta}d\left(\frac{x}{L}\right)\Big/\left(\frac{dL}{d\theta}\cdot\frac{x}{L}\right) \tag{5. 4}$$

The overall material balance in filtration is written as

$$L=\frac{(m-1)s}{\varepsilon_{av}(1-ms)}v \tag{5. 5}$$

where m is the ratio of wet to dry cake mass and $m=1+\rho\varepsilon_{av}/\{\rho_s(1-\varepsilon_{av})\}$.

Differentiating Eq. (5.5) with respect to time, one gets

$$\frac{dL}{d\theta}=\frac{(m-1)\rho}{\varepsilon_{av}(1-ms)}\left\{q_1+v\left(\frac{\varepsilon_{av}}{m-1}+\frac{s}{1-ms}\cdot\frac{dm}{d\theta}\right)\right\} \tag{5.6}$$

Combination of Eqs. (5.3) and (5.6) yields the expression for variation q:

$$\frac{q}{q_1}=1-\frac{(\varepsilon-\varepsilon_{av\cdot x}-E)(m-1)}{\varepsilon_{av}(1-ms)}s\frac{x}{L}\left\{1+\frac{v}{q_1}\left(\frac{\varepsilon_{av}}{m-1}+\frac{s}{1-ms}\cdot\frac{dm}{d\theta}\right)\right\} \tag{5.7}$$

For constant pressure filtration under the condition of negligible medium resistance, ε is a function of x/L alone,[19] and Eq. (5.7) reduces to Eq. (2.24) by placing $dm/d\theta=0$ and $E=0$.

Rigorous solutions for constant rate and variable pressure-variable rate filtration operations should be analyzed on the basis of Eq. (5.7). However, using Eq. (5.7) may present great difficulties because of its complexity. On the assumption that the rate of increase of filtration pressure is not so large, both $dm/d\theta$ and E become zero in the neighborhood of a specified filtration time. The calculations can be executed by using Eq. (2.24), instead of Eq. (5.7). Therefore, one can follow mathematical procedures which are similar to the case of constant pressure filtration when predicting various filtration characteristics for an arbitrary pressure drop $(p-p_m)$ across the cake during a filtration operation.

5. 3. *Constant rate filtration*

From an overall viewpoint, a material balance can be written as

$$w_0=\frac{\rho s}{1-ms}v \tag{5.8}$$

Substituting $v=q_1\theta$ into Eq. (5.8) and combining the result with Eq. (2.29) gives the p vs. θ relation at the constant rate filtration:

$$\theta=\frac{1-ms}{\mu\alpha_{av}\rho s q_1^2}(p-p_m) \tag{5.9}$$

On the assumption that the filtration characteristics will have approximately the same values for the same pressure drop across the cake in both cnnstant pressure and constant rate operation, the p vs. θ relation at the constant rate filtration can be calculated from Eq. (5.9).

The apparatus used in constant rate filtration is based upon a modification of a bomb filter commonly used with several devices for filtration at exactly constant rate. Figure 5. 1 shows the schematic picture of the experimental apparatus. It consists mainly of a bomb filter equipped with a stuffing box, a long piston and a

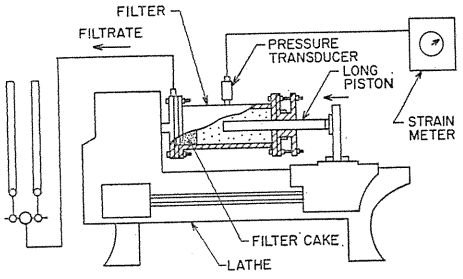

Fig. 5. 1. Schematic diagram of experimental apparatus for constant rate filtration.

device for driving the piston at constant velocity. Filtration pressure is applied to the slurry in the bomb through the piston which is forced at a constant speed into the filter by the tool post of a machine lathe, and the filtration is carried out exactly at a constant rate. The filtration pressure at any time θ can be measured by a force transducer, with accompanying strain gauges.

In Figs. 5. 2 and 5. 3, v and p vs. θ data obtained from constant rate filtration experiments are illustrated. In the same figure, the predicted results calculated from Eq. (5. 9) are also plotted. Figure 5. 2 shows experimental results for a small rate of increase of filtration pressure and Fig. 5. 3 shows that for rapid increase of filtration pressure. It is apparent from Fig. 5. 2 that the calculations are fairly consistent with the experimental results, whereas Fig. 5. 3 shows poor agreement between calculations and experiments. The discrepancy is probably attributable to the fact that it is unreasonable to put $dm/d\theta=0$ and $E=0$ in Eq. (5. 7) and that ultimate values of porosity are not attained instantaneously because of rapid increase of filtration pressure.

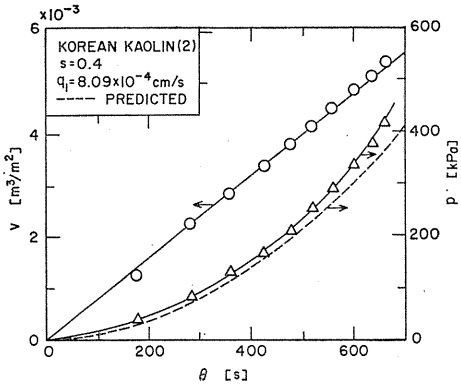

Fig. 5. 2. Constant rate filtration result for small rate of increase of filtration pressure.

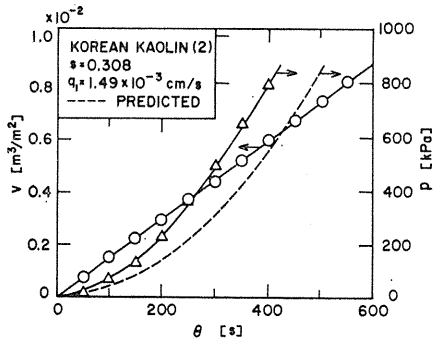

Fig. 5. 3. Constant rate filtration result for rapid increase of filtration pressure.

5. 4. Variable pressure-variable rate filtration

Combining Eq. (2. 29) with Eq. (5. 8), one gets

$$p-p_m=\frac{\mu\alpha_{av}\rho s q_1}{1-ms}v \tag{5. 10}$$

For variable pressure-variable rate filtration, provided that the relation of $(p-p_m)$ vs. v is given, the relation of q_1 vs. v can be obtained from Eq. (5. 10), and vice versa. Once the relation of $1/q_1\equiv d\theta/dv$ vs. v has been determined, the time θ can be obtained from the following integral:

$$\theta=\int_0^v\frac{d\theta}{dv}dv=\int_0^v\frac{1}{q_1}dv \tag{5. 11}$$

Figure 5. 4 represents the discharge characteristics of the pump used for the

variable pressure-variable rate filtration experiment. Provided the values of α_{av} and m for various values $(p-p_m)$ are given, the relationship of p vs. q_1 for various values of v can be obtained using Eq. (5. 10). In the same figure, the theoretical curve of p vs. q_1, with v as a parameter, is superimposed. The points of intersection of p vs. q_1 curve with the discharge characteristic curve of the pump give the relation between q_1 and v. The relation of $1/q_1$ vs. v thus determined is illustrated in Fig. 5. 5. Figure 5. 6 represents the relation of v vs. θ obtained by graphical integration of $1/q_1$ vs. v in Fig. 5. 5.

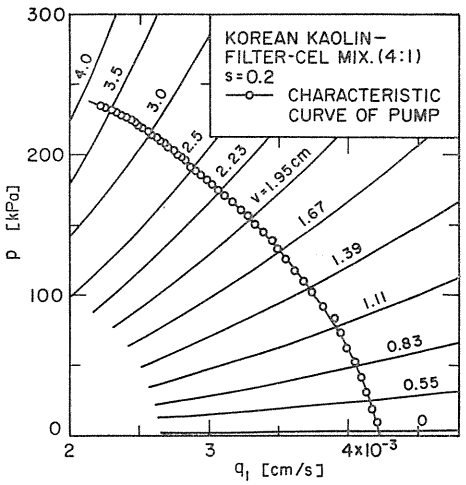

Fig. 5. 4. p vs. q_1 of variable pressure-variable rate filtration and of pump characteristics.

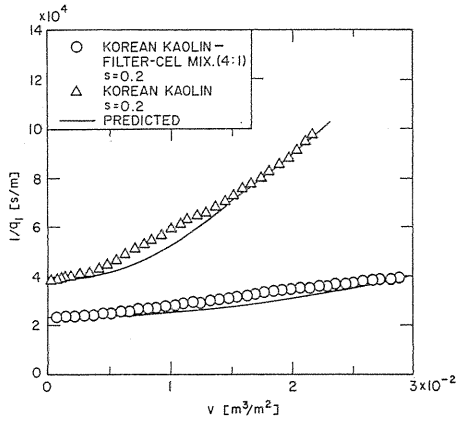

Fig. 5. 5. Relation between $1/q_1$ and v.

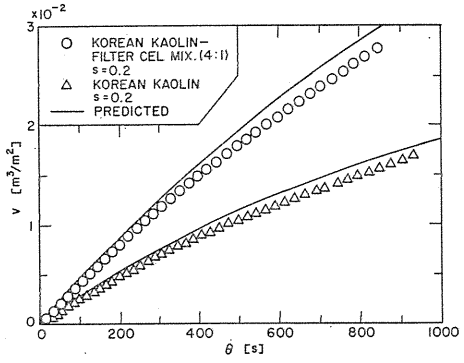

Fig. 5. 6. Relation between filtrate volume and filtration time.

6. Non Uni-Dimensional Filtration

6. 1. Introduction

The previous filtration equations have generally assumed constant filtration area, which is only maintained where there is a retaining wall that forces uni-dimensional cake deposition. Filtration, as practiced in industry, however, is not always a simple, uni-dimensional phenomenon. If a cake is deposited either internally or externally on a cylindrical element, any substantial change in cake thickness will vary the filtration area. In a leaf filter, the area grows as the cake extends

beyond the medium.

The industrially important area of non uni-dimensional filtration has been virtually untouched. While some work has been done to account for non uni-dimensional cake, only an ideal case in three-dimensional filtration on a circular leaf has been studied by Brenner.[46,47] Applying Brenner's work, the present authors have developed a term, "effective filtration area factor j_N".

Starting from the basic differential equations for flow through porous media, non uni-dimensional filtration theories are developed in terms of the effective filtration area factor j_N. In this chapter, theoretical and experimental methods are presented for obtaining values of j_N for two-dimensional filtration on cylindrical (tubular) surfaces and three-dimensional filtration on spherical surfaces.[22~24]

6. 2. Relations between hydraulic and compressive pressure

In order to derive the relation between local values of p_L and p_s in non uni-dimensional cake, a two-dimensional cake on a cylindrical filter surface will be considered.[25] As a first basic postulate, it is assumed that the particles in the cake are in point contact and communicate the compressive pressure $k_0 p_s$, where k_0 is a coefficient of earth pressure,[48] in a direction along a plane perpendicular to the direction of p_s, and that the liquid completely bathes each particle and communicates the liquid pressure p_L uniformly in a direction along a plane perpendicular to the direction of flow. Under this assumption, the net force on the total mass within the differential volume element AA'B'B (Fig. 6. 1) may be described in detail. The hydraulic pressure p_L and the solid compressive pressure p_s being effective over the entire cross sections of the differential element of cake, the force F acting on the side of the differential area AB is given by

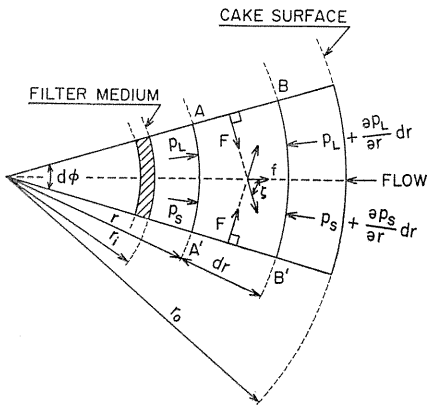

Fig. 6. 1. Differential volume element of cylindrical filter cake.

$$F=\left\{\left(p_L+\frac{1}{2}\cdot\frac{\partial p_L}{\partial r}dr\right)+k_0\left(p_s+\frac{1}{2}\cdot\frac{\partial p_s}{\partial r}dr\right)\right\}hdr \tag{6.1}$$

where r is the radius and h the height of the differential volume element. The resultant force f in the direction of flow is given by

$$\begin{aligned} f&=-2F\cos\zeta=-2F\cos\left(\frac{\pi}{2}-\frac{d\phi}{2}\right)=-2F\sin\left(\frac{d\phi}{2}\right)\\ &=-Fd\phi\\ &=-\left\{\left(p_L+\frac{1}{2}\cdot\frac{\partial p_L}{\partial r}dr\right)+k_0\left(p_s+\frac{1}{2}\cdot\frac{\partial p_s}{\partial r}dr\right)\right\}hdrd\phi \end{aligned} \tag{6.2}$$

where the positive direction of force is taken in accordance with the direction of

flow, andϕ and ζ are the angles as denoted in Fig. 6.1. The forces exerted on the two cylindrical surfaces, AA′ and BB′, are

$$F_r = -(p_L + p_s) h r d\phi \tag{6.3}$$

and

$$F_{r+dr} = -\left(F_r + \frac{\partial F_r}{\partial r} dr\right)$$

$$= (p_L + p_s) h r d\phi + \left\{\left(\frac{\partial p_L}{\partial r} + \frac{\partial p_s}{\partial r}\right) r + (p_L + p_s)\right\} h dr d\phi \tag{6.4}$$

respectively. The forces acting on the planes, AA′ and BB′, being equal and in opposite direction, cancel one another. The net force on the total mass within the differential element is now given by

$$\text{Net force} = f + F_r + F_{r+dr} \tag{6.5}$$

This force equals the product of the mass within the differential element and the acceleration. The differential mass includes the mass of both liquid and solids. Under the assumption of negligible acceleration of solids and liquid,[49] Eq. (6.5) can be written as

$$f + F_r + F_{r+dr} = 0 \tag{6.6}$$

or

$$\frac{\partial p_L}{\partial r} + \frac{\partial p_s}{\partial r} + (1 - k_0) \frac{p_s}{r} = 0 \tag{6.7}$$

Integration of Eq. (6.7) and use of the boundary conditions $p_L = p$ (applied filtration pressure) and $p_s = 0$ at the cake surface $r = r_0$ gives

$$p_L + p_s = p + \int_r^{r_0} \frac{(1 - k_0) p_s}{r} dr \tag{6.8}$$

If the solid particles in the cake are very fine (smaller than about 5 μm) and the cohesive force between the particles is negligible, the coefficient k_0 of cake compressive pressure equals nearly one,[48] and, consequently, Eq. (6.8) yields Eq. (3.4). According to the same arguments as mentioned above, Eq. (3.4) may be derived for various non uni-dimensional cakes.

It should be noted that the compressive pressure p_s is defined as the pressure of the compressive force divided by the total sectional area. Collins[50] has derived Eq. (3.4) in view of all forces acting on the solids in a uni-dimensional cake, and has mentioned that Tiller[49] did not include a viscous drag term due to fluid motion and by a fortuitous circumstance his final result was the same as that derived by him.[50] However, it should be emphasized that the analysis attempted by Tiller and authors is based upon the net force on the total mass of a differential volume, and not only on the solids as attempted by Collins.

6. 3. Fundamental equations for non uni-dimensional filtration

Using vector notation, a basic non uni-dimensional flow equation through compressible porous media can be written as[14, 23]

$$\boldsymbol{u}=\frac{\boldsymbol{q}}{\varepsilon}-\frac{\boldsymbol{r}}{1-\varepsilon} \quad \text{or} \quad \varepsilon\boldsymbol{u}=\boldsymbol{q}-\frac{\varepsilon\boldsymbol{r}}{1-\varepsilon}=\boldsymbol{q}-e\boldsymbol{r} \tag{6.9}$$

where $\boldsymbol{u}$ is the local value of the relative velocity of liquid to solids, $\boldsymbol{q}$ the local apparent velocity of liquid and $\boldsymbol{r}$ the local apparent velocity of solids. Actually, $\boldsymbol{u}$, $\boldsymbol{q}$, $\boldsymbol{r}$, ε and e are functions of position and time. Since $\varepsilon\boldsymbol{u}$ is the apparent relative velocity of liquid to solids, the above equation can be rewritten as

$$\varepsilon\boldsymbol{u}=\boldsymbol{q}-e\boldsymbol{r}=-\frac{1}{\mu\alpha(1-\varepsilon)\rho_s}\text{grad}\ p_L \tag{6.10}$$

For an incompressible cake, $\boldsymbol{r}$ equals zero and Eq. (6. 10) becomes[46]

$$\boldsymbol{q}=-\frac{1}{\mu\alpha(1-\varepsilon)\rho_s}\text{grad}\ p_L=-\frac{k}{\mu}\text{grad}\ p_L \tag{6.11}$$

where k is the permeability coefficient, represented by

$$k=\frac{1}{\alpha(1-\varepsilon)\rho_s}=\text{const.} \tag{6.12}$$

All problems in fluid flow require that the continuity equation be satisfied. The equation for a non uni-dimensional flow through compressible media can be generally represented as

$$\frac{\partial(\rho\varepsilon)}{\partial\theta}+\text{div}(\rho\boldsymbol{q})=0 \tag{6.13}$$

The liquid being incompressible, Eg. (6. 13) becomes[13, 14]

$$\frac{\partial\varepsilon}{\partial\theta}+\text{div}\ \boldsymbol{q}=0 \tag{6.14}$$

In accordance with the same procedure as mentioned above, the continuity equation of solids may be represented in the following form[14]

$$-\frac{\partial\varepsilon}{\partial\theta}+\text{div}\ \boldsymbol{r}=0 \tag{6.15}$$

Substitution of Eq. (6. 15) into Eq. (6. 14) gives

$$\text{div}(\boldsymbol{q}+\boldsymbol{r})=0 \tag{6.16}$$

For an incompressible cake, Eq. (6. 16) becomes

$$\text{div}\ \boldsymbol{q}=0 \tag{6.17}$$

Substitution of Eq. (6. 11) into Eq. (6. 17) leads to

$$\mathrm{div}\left(-\frac{k}{\mu}\mathrm{grad}\ p_L\right)=-\frac{k}{\mu}\mathrm{div}(\mathrm{grad}\ p_L)=0$$

or

$$\nabla^2 p=0 \tag{6.18}$$

where ∇^2 is the so-called Laplacian operator.

In order to obtain the solution for a non uni-dimensional problem in a specified coordinate system, the pressure variation is calculated from Eq. (6.18), and the flow variation determined by Eq. (6.11). It should be added that the cake profile coincides with the equi-pressure surface and the flow pattern of filtrate follows potential flow pathlines.

6. 4. Two-dimensional filtration on cylindrical geometries

In order to obtain useful equations for practical design without making the analysis unduly complex, it is assumed that the filter cakes are incompressible and that the filter media offer no resistance to the flow of filtrate through them. The problem of determining the cake deposition on a cylindrical element as a function of time is best discussed in a system of the cylindrical coordinates (r, ϕ, z), as shown in Fig. 6.2. The equi-presssure surface within the cake being identical with the cylindrical surface of a constant radius r, that is $p_L=p_L\ (r, \theta)$, one obtains

$$\nabla^2 p_L=\frac{1}{r}\cdot\frac{\partial}{\partial r}\left(r\frac{\partial p_L}{\partial r}\right)=0 \tag{6.19}$$

Integrating the above equation and substituting both the boundary conditions ($p_L=p_i$ at the medium surface $r=r_i$, and $p_L=p_0$ at the cake surface $r=r_0$) and the initial condition ($r=r_0=r_i$ at $\theta=0$), one gets

$$p_L=p_0+(p_0-p_i)\frac{\ln(r/r_0)}{\ln(r_0/r_i)} \tag{6.20}$$

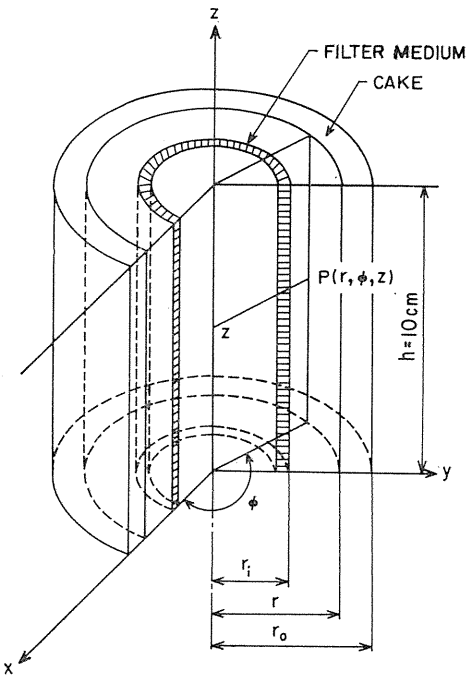

Fig. 6. 2. Cake on cylindrical filter element.

Differentiating the above equation partially with respect to r and substituting the derivative into Eq. (6.11) leads to

$$q=|\boldsymbol{q}|=\frac{k}{\mu}\cdot\frac{1}{r}\cdot\frac{p}{\ln(r_0/r_i)} \tag{6.21}$$

where p is the filtration pressure and $p=p_0-p_i=$ const.

Of primary interest is the velocity of filtrate at the filter medium $r=r_i$.

This is easily found by setting $r=r_i$ in Eq. (6.21).

$$\left(\frac{dv}{d\theta}\right)=q|_{r=r_i}=\frac{k}{\mu}\cdot\frac{1}{r_i}\cdot\frac{p}{\ln(r_0/r_i)}$$

$$=\frac{1}{\alpha(1-\varepsilon)\rho_s}\cdot\frac{p}{\mu r_i\ln(r_0/r_i)} \tag{6.22}$$

The volume V_c of the filter cake is given by

$$V_c=v_cA=\pi h(r_0^2-r_i^2) \tag{6.23}$$

where h is the length of the cylindrical element and A the filter-medium area ($A=2\pi r_ih$). The total mass of dry cake per unit filter-medium area w_0 ($w_0=W_0/A$) is given by

$$w_0=\frac{V_c}{A}\rho_s(1-\varepsilon)=\frac{r_i}{2}\left\{\left(\frac{r_0}{r_i}\right)^2-1\right\}\rho_s(1-\varepsilon) \tag{6.24}$$

Substituting Eq. (6.24) in Eq. (6.22), one obtains

$$\left(\frac{dv}{d\theta}\right)_{\mathrm{II},\,cy}=\frac{1}{2}\left\{\left(\frac{r_0}{r_i}\right)^2-1\right\}\frac{1}{\ln(r_0/r_i)}\cdot\frac{p}{\mu\alpha_{av}w_0}$$

$$=\frac{2(v_c/r_i)}{\ln\{1+2(v_c/r_i)\}}\cdot\frac{p}{\mu\alpha_{av}w_0} \tag{6.25}$$

Equation (6.25) represents the flow rate of filtrate for the two-dimensional filtration on a cylindrical element at a constant pressure and the subscript $(dv/d\theta)_{\mathrm{II},\,cy}$ is employed.

6.5. *Effective filtration area factor*

The conventional uni-dimensional form of Ruth's equation of filtration with a negligible septum resistance is written as

$$\left(\frac{dv}{d\theta}\right)_{\mathrm{I}}=\frac{p}{\mu\alpha_{av}(W_0/A)}=\frac{p}{\mu\alpha_{av}w_0} \tag{6.26}$$

This equation requires modification if the area growth is appreciable. Comparison with Eq. (6.25) shows that Eq. (6.25) is a modified form of Ruth's equation for filtration on a cylindrical element. In order to obtain a useful mathematical tool for non uni-dimensional filtration, it appears advantageous to modify Eq. (6.26) as

$$\left(\frac{dv}{d\theta}\right)_N=\frac{p}{\mu\alpha_{av}\dfrac{W_0}{A_e}}=\frac{p}{\mu\alpha_{av}\dfrac{W_0}{A}\cdot\dfrac{A}{A_e}}=\frac{p}{\mu\alpha_{av}\dfrac{w_0}{j_N}} \tag{6.27}$$

where the subscript N is employed to emphasize that the equation can be used for general problems of both uni-dimensional and non uni-dimensional filtrations, and A_e denotes the effective filtration area defined by Eq. (6.27), and j_N is the effective filtration area factor defined by

$$j_N=\frac{A_e}{A}=\left[\frac{(dv/d\theta)_N}{(dv/d\theta)_{\mathrm{I}}}\right]_{w_0}=\left[\frac{(d\theta/dv)_{\mathrm{I}}}{(d\theta/dv)_N}\right]_{w_0} \tag{6.28}$$

It is apparent that the values of j_N can be well determined analytically and experimentally by Eq. (6.28) at an equal value of w_0 or v_c.

In accordance with the definition of j_N, the effective area factor for the two-dimensional filtration on a cylindrical surface can be represented as

$$j_{\mathrm{II},cy}=\frac{1}{2}\left\{\left(\frac{r_0}{r_i}\right)^2-1\right\}\frac{1}{\ln(r_0/r_i)}=\frac{2(v_c/r_i)}{\ln\{1+2(v_c/r_i)\}} \tag{6.29}$$

The effective area factor being known, the flow rate $(dv/d\theta)_{\mathrm{II},cy}$ at any specified value of w_0 can be calculated from Eq. (6.27) and the time-volume relation may be easily obtained.

Starting from the basic Eqs. (6.11) and (6.18), one can obtain the filtration area factor j_N for any specified coordinate system in accord with the same mathematical procedure mentioned before. In the cases of some typical non uni-dimensional filtration problems, the results are now summarized.

(i) Uni-dimensional filtration:

$$j_{\mathrm{I}}=1 \tag{6.30}$$

(ii) Two-dimensional filtration on cylindrical element (Fig. 6.2):

$$j_{\mathrm{II},cy}=\frac{\pm 2\dfrac{v_c}{r_i}}{\ln\left(1\pm 2\dfrac{v_c}{r_i}\right)},\quad \begin{matrix}+\ ;\ r_0\geqq r_i\\ -\ ;\ r_0\leqq r_i\end{matrix} \tag{6.31}$$

(iii) Three-dimensional filtration on spherical leaf (Fig. 6.3):

$$j_{\mathrm{III},sp}=\frac{1}{3}\left\{\left(1\pm 3\frac{v_c}{r_i}\right)+\left(1\pm 3\frac{v_c}{r_i}\right)^{\frac{2}{3}}+\left(1\pm 3\frac{v_c}{r_i}\right)^{\frac{1}{3}}\right\},\quad \begin{matrix}+\ ;\ r_0\geqq r_i\\ -\ ;\ r_0\leqq r_i\end{matrix} \tag{6.32}$$

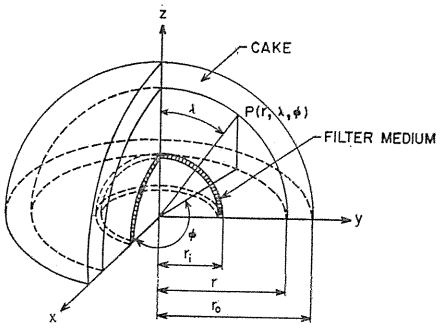

Fig. 6. 3. Cake on spherical filter element.

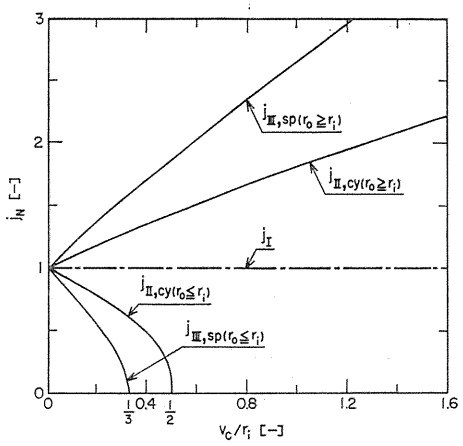

Fig. 6. 4. Theoretical values of $j_{\mathrm{II},cy}$ and $j_{\mathrm{III},sp}$.

In Fig. 6. 4, the analytical values of j_N are illustrated.

6. 6. Experimental equipment and results

For studying the problems of non uni-dimensional filtration, cylindrical elements of radius r_i=1. 25, 2. 50, 3. 75 and 5. 00 (Fig. 6. 2) are used. The schematic picture of the experimental apparatus is shown in Fig. 6. 5.

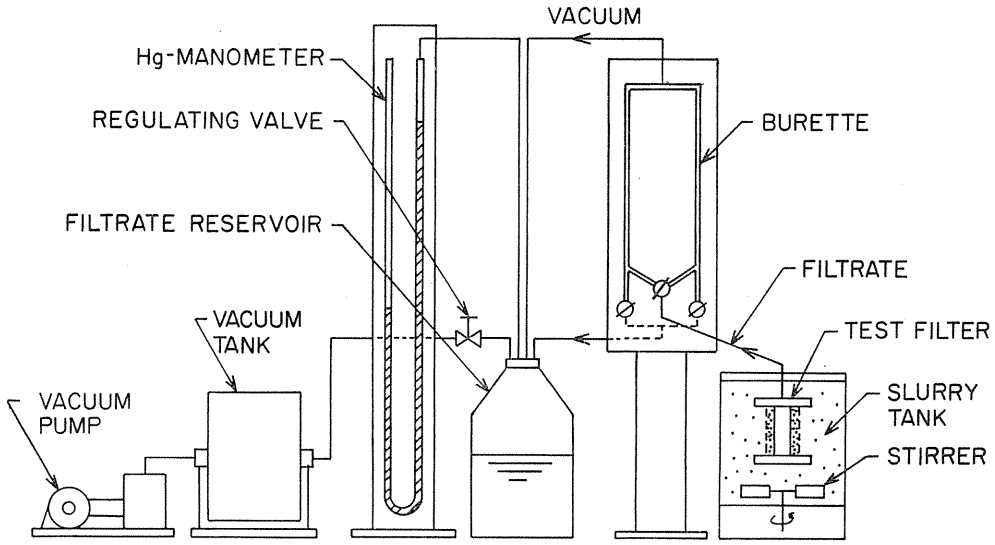

Fig. 6. 5. Schematic diagram of experimental apparatus.

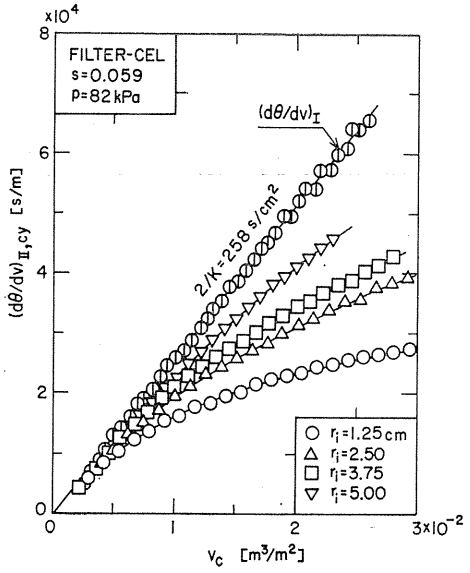

Fig. 6. 6. Relation between $(d\theta/dv)_{\mathrm{II},cy}$ and v_c for filtration on cylindrical element.

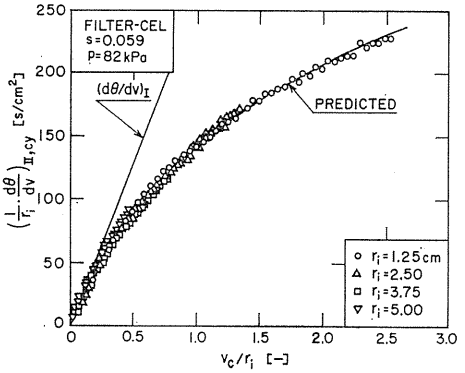

Fig. 6. 7. Relation between $(1/r_i \cdot d\theta/dv)_{\mathrm{II},cy}$ and v_c/r_i for filtration on cylindrical element.

Figure 6.6 shows experimental data of $(d\theta/dv)_{\text{II,cy}}$ vs. v_c, together with unidimensional filtration data. It is apparent that $[(1/r_i)\ (d\theta/dv)]_{\text{II,cy}}$ vs. v_c/r_i represents a unique relation as may be seen from Fig. 6.7 or Eq. (6.22).

The experimental values of j_N can be well determined from experimental values of $(dv/d\theta)_{\text{I}}$ and $(dv/d\theta)_N$ on the basis of Eq. (6.28). The experimental j_N-values thus obtained compare favorably with the theoretical j_N-values illustrated in Fig. 6.8.

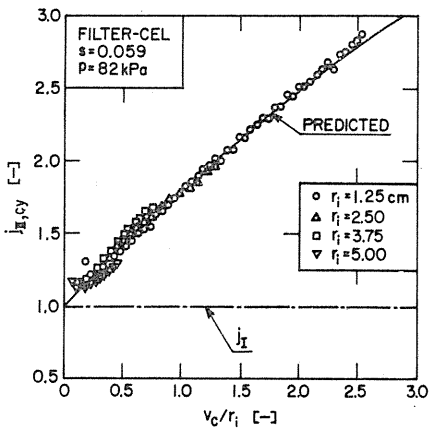

Fig. 6.8. Relation between $j_{\text{II,cy}}$ and v_c/r_i.

7. Filtration of Non-Newtonian Fluids

7.1. Introduction

Filtration of non-Newtonian fluid-solid mixtures is a subject of great importance in many diversified fields as the petrochemical and food processing industries. In non-Newtonian filtration, the filtrate is a non-Newtonian fluid. If the filtrate shows the behavior of a pseudo-plastic fluid, an empirical functional relation known as the so-called power-law can be used to represent its fluid behavior. This relation may be written as

$$\tau = K\dot{\gamma}^N \tag{7.1}$$

where τ is the shear stress, K the fluid consistency index, $\dot{\gamma}$ the shear rate and N the flow behavior index. The latter is a measure of the degree of non-Newtonian behavior of the fluid, and the greater the departure from unity the more the fluid behavior deviates from Newtonian behavior (that is, the fluid is more non-Newtonian). Equation (7.1) can be rearranged into the form

$$f(\tau) \equiv \dot{\gamma} = \left(\frac{\tau}{K}\right)^{\frac{1}{N}} \tag{7.2}$$

Kozicki et al.,[51,52] and Shirato et al.[26~30,53,54] developed non-Newtonian filtration theories for power-law fluid-solid mixtures.

7.2. Overall filter cake characteristics of non-Newtonian filtration

The generalized Rabinowitch Mooney equation (Eq. (7.3) below) serves as the basis for the flow of time-independent non-Newtonian fluids through geometries of arbitrary cross section and, as such, represents the basis for non-Newtonian filtration analysis. This equation is given by

$$\frac{2U_e}{r_H}=\frac{1}{a}\tau_w^{-\frac{b}{a}}\int_0^{\tau_w}\tau^{\frac{b}{a}-1}f(\tau)\,d\tau \tag{7.3}$$

where U_e is the average flow rate, r_H the hydraulic radius, a and b are geometric constants depending on the cross-sectional shapes of the ducts and τ_w the shear stress at the wall. When Eq. (7.3) is applied to flow through granular beds, U_e must be the real flow rate along with the actual sinuous path through the bed, and can be related to the apparent velocity U and the bed tortuosity T by:

$$U_e=TU \tag{7.4}$$

The tortuosity is the ratio of length of the actual flow path to the length of the bed, and the value $T=\sqrt{2}$ is recommended by Carman.[10] Substituting Eqs. (7.1) and (7.4) into Eq. (7.3) and integrating yields

$$U=\frac{(1+\xi)N}{1+\xi N}\cdot\frac{r_H}{TK_0}\left(\frac{\tau_w}{K}\right)^{\frac{1}{N}} \tag{7.5}$$

where

$$K_0=2(a+b) \tag{7.6}$$

$$\xi=b/a \tag{7.7}$$

Kozicki et al.[55] pointed out that ξ, the aspect factor, is 3.0 for the usual granular bed, the same as for circular conduits. The impermeability K_0 is related to Kozeny's constant k by the equation:

$$k=T^2K_0 \tag{7.8}$$

For filtrate flow in filter cakes, U in Eq. (7.5) represents the relative velocity of liquid with respect to migrating solids, and is related to the apparent liquid velocity u relative to solids by

$$U=u/\varepsilon \tag{7.9}$$

The force balance between the shear stress τ_w on the solids and the hydraulic pressure loss dp_L through a differential cake thickness dx gives

$$\tau_w=\frac{r_H}{T}\cdot\frac{dp_L}{dx} \tag{7.10}$$

where

$$r_H=\frac{\varepsilon}{S_0(1-\varepsilon)} \tag{7.11}$$

When representing an arbitrary position in a filter cake during filtration, a variable ω, the volume of solids per unit cross-sectional area measured from the cake bottom, can be used instead of the conventional fixed-coordinate distance x. In compressible cake filtration, the actual position in the cake corresponding to any value of ω changes with time θ due to solids migration.[56] The volume $d\omega$ is

related to dx by

$$d\omega=(1-\varepsilon)dx \tag{7.12}$$

It should be noted that the solutions are the same, starting either from the fixed-coordinate, or from the moving-coordinate.

Substituting Eqs. (7.8) ~ (7.12) into Eq. (7.5), the basic flow equation for filtration of a power-law fluid-solid mixtures can be expressed in the form

$$u^N=\frac{1}{K\gamma\rho_s}\cdot\frac{\partial p_L}{\partial\omega}=-\frac{1}{K\gamma\rho_s}\cdot\frac{\partial p_s}{\partial\omega} \tag{7.13}$$

where

$$\gamma\equiv\left\{\frac{1+\xi N}{(1+\xi)N}\right\}\left\{\frac{T\varepsilon^2}{kS_0(1-\varepsilon)}\right\}^{1-N}\alpha \tag{7.14}$$

γ is the local specific filtration resistance for power-law fluids and α is the local specific filtration resistance for Newtonian filtration defined by Eq. (3.9).

Since $p_s=0$ at the cake surface where $\omega=\omega_0$, and $p_s=p-p_m$ at the cake bottom where $\omega=0$, Eq. (7.13) can be integrated over the cake thickness to obtain (after some rearrangement):

$$u_1{}^N\equiv\left(\frac{dv}{d\theta}\right)^N=\frac{p-p_m}{K\rho_s\gamma_{av}\omega_0}=\frac{p}{K(\rho_s\gamma_{av}\omega_0+R_m)} \tag{7.15}$$

where u_1 is the u-value at the cake bottom, which is identical with conventional filtration velocity, ω_0 the solids volume of the entire cake per unit area and γ_{av} the average specific filtration resistance for power-law non-Newtonian fluids defined by

$$\gamma_{av}=J_{gen}\gamma_K \tag{7.16}$$

where

$$J_{gen}\equiv\int_0^1\left(\frac{u}{u_1}\right)^N d\left(\frac{\omega}{\omega_0}\right) \tag{7.17}$$

$$\gamma_K\equiv(p-p_m)/\int_0^{p-p_m}\frac{1}{\gamma}dp_s \tag{7.18}$$

where γ_K is an approximation of average specific filtration resistance, which is virtually the same as presented by Kozicki et al.,[51] and J_{gen} is a correction factor by which γ_K should be multiplied.

In order to obtain u/u_1 in Eq. (7.17), assume a differential cake slice $d\omega$ bounded by the ω- and $(\omega+d\omega)$- planes within a filter cake. In the subsequent derivation, it is essential to recognize that the movement of the ω- or $(\omega+d\omega)$-planes is identical with that of solid particles located in the ω- or $(\omega+d\omega)$-positions, respectively, and the filtrate velocity across the ω-plane is the relative liquid velocity with respect to solids, u. Denoting the local void ratio by e, one can write a material balance over $d\omega$ on unit area basis to obtain

$$\left(u+\frac{\partial u}{\partial \omega}d\omega\right)d\theta-ud\theta=\frac{\partial e}{\partial \theta}d\theta d\omega$$

from which, the continuity equation is obtained:

$$\partial u/\partial \omega=\partial e/\partial \theta \tag{7.19}$$

To solve Eq. (7.19) analytically under constant pressure conditions, it is necessary to assume that the local void ratio e is a function of ω/ω_0 alone,[19] and consequently, the average void ratio of entire cake e_{av} is constant.

Under the above assumption, integration of Eq. (7.19) leads to

$$\frac{u}{u_1}=1-\frac{(e-e_{av\cdot\omega})(m-1)}{e_{av}(1-ms)}s\frac{\omega}{\omega_0} \tag{7.20}$$

where $e_{av\cdot\omega}$ is the average void ratio over the range from 0 to ω as defined by

$$e_{av\cdot\omega}\equiv\frac{1}{\omega}\int_0^{\omega}e(\omega,\ \theta)d\omega=\frac{1}{\omega/\omega_0}\int_0^{\omega/\omega_0}e(\omega/\omega_0)d\left(\frac{\omega}{\omega_0}\right) \tag{7.21}$$

The average void ratio over the entire cake, e_{av}, can be defined in the same manner, i. e.,

$$e_{av}\equiv\frac{1}{\omega_0}\int_0^{\omega_0}e(\omega,\ \theta)d\omega=\int_0^1 e(\omega/\omega_0)d\left(\frac{\omega}{\omega_0}\right) \tag{7.22}$$

The values of J_{gen} are shown in Fig. 7.1. In non-Newtonian filtration, the slurry concentration has relatively little effect, even for concentrated slurries of compressible materials, which is in contrast to Newtonian filtration.

It is assumed that compression-permeability cell data on the water suspension may serve as the basic tool for the analysis of non-Newtonian filtration. In Fig. 7.2, the average specific resistance based upon Eq. (7.16) and compression-permeability data is shown as a function of N, $(p-p_m)$ and s. The average specific resistances are strongly dependent on the flow behavior index N and are only weakly dependent on $(p-p_m)$ and s.

From an overall viewpoint, a material balance can be written as

$$\omega_0=\frac{\rho s}{\rho_s(1-ms)}v \tag{7.23}$$

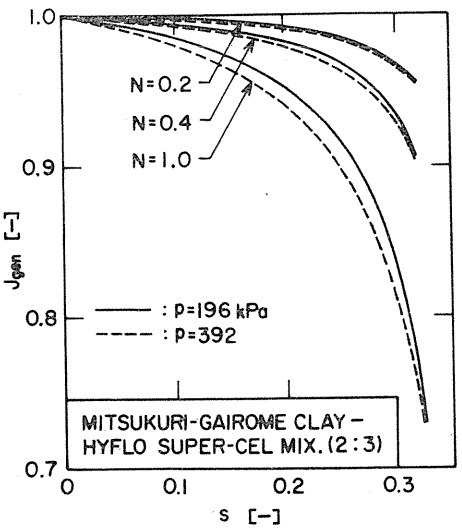

Fig. 7. 1. Effect of s and N on J_{gen}.

Combining Eq. (7.15) with Eq. (7.23) in accordance with concept of the fictitious filtrate volume v_m corresponding to medium resistance, yields

$$\left(\frac{1}{u_1}\right)^N \equiv \left(\frac{d\theta}{dv}\right)^N = \frac{K\gamma_{av}\rho s(v+v_m)}{p(1-ms)} \tag{7.24}$$

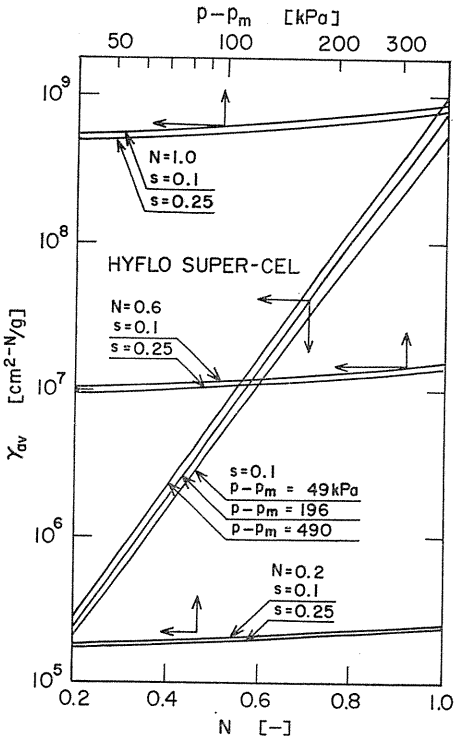

Fig. 7. 2. Effect of N, $(p-p_m)$ and s on γ_{av}.

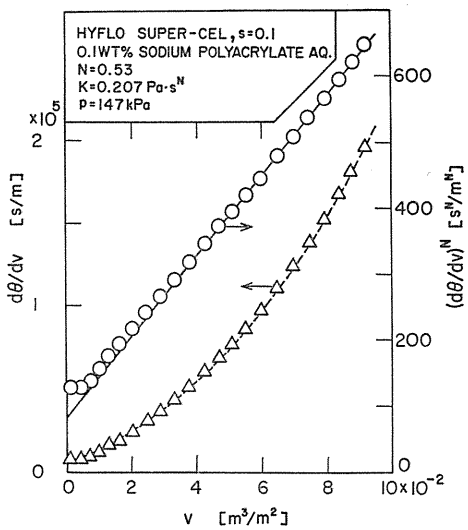

Fig. 7. 3. Variation of $d\theta/dv$ and $(d\theta/dv)^N$ with v.

In Fig. 7. 3, $d\theta/dv$ is plotted against filtrate volume v for constant pressure filtration. Hyflo Super-Cel, a typical diatomaceous filter aid, is used as the solid material. The liquid is an aqueous solution of sodium polyacrylate. The $d\theta/dv$ vs. v data exhibit a behavior which is concave upwards. In the same figure, $(d\theta/dv)^N$ is plotted against v for the same run. In this case, $(d\theta/dv)^N$ vs. v shows a linear relationship in accordance with the theory indicated by Eq. (7. 24) since γ_{av} and m are constant for constant pressure filtration.

It is possible to integrate Eq. (7. 24) for constant pressure filtration to obtain

$$(v+v_m)^{(1+N)/N} = K_N(\theta+\theta_m) \tag{7.25}$$

where K_N is the non-Newtonian filtration coefficient under constant pressure, and is defined by

$$K_N \equiv \frac{1+N}{N}\left\{\frac{p(1-ms)}{K\rho s\gamma_{av}}\right\}^{1/N} \tag{7.26}$$

and the fictitious filtration time θ_m corresponding to the medium resistance is

defined by

$$\theta_m \equiv K_N^{-1} v_m^{(1+N)/N} \qquad (7.27)$$

The time-volume relations which are determined by the theoretical calculations and the filtration experiments are compared in Fig. 7.4.

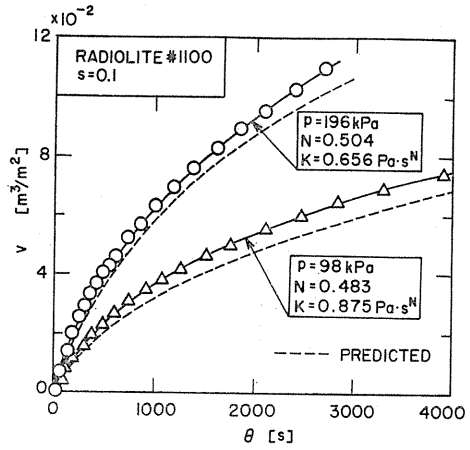

Fig. 7.4. Relation between filtrate volume and filtration time.

7.3. Internal flow mechanism in non-Newtonian filter cake

Integrating Eq. (7.13) over the range from 0 to ω and also 0 to ω_0 (the entire cake), respectively, and combining the results yields

$$\frac{p_L - p_m}{p - p_m} = 1 - \frac{p_s}{p - p_m} = \frac{\int_0^{\omega/\omega_0} \left(\frac{u}{u_1}\right)^N \gamma d\left(\frac{\omega}{\omega_0}\right)}{\int_0^1 \left(\frac{u}{u_1}\right)^N \gamma d\left(\frac{\omega}{\omega_0}\right)} \qquad (7.28)$$

or

$$1 - \frac{\int_0^{p_m} \frac{1}{\gamma} dp_s}{\int_0^{p-p_m} \frac{1}{\gamma} dp_s} = \frac{\int_0^{\omega/\omega_0} \left(\frac{u}{u_1}\right)^N d\left(\frac{\omega}{\omega_0}\right)}{\int_0^1 \left(\frac{u}{u_1}\right)^N d\left(\frac{\omega}{\omega_0}\right)} \qquad (7.29)$$

The local specific resistance γ depends on p_s alone as is obvious from its definition; whereas u/u_1 depends on the solid compressive pressure distribution as indicated by Eq. (7.20). Equations (7.28) or (7.29) provide a relationship between the solid compressive pressure p_s and the fractional solid volume ω/ω_0 through the cake under a given $(p-p_m)$ condition.

With the aid of both Eq. (7.20) and compression-permeability tests, Eq. (7.28) or (7.29) serves as the theory for predicting internal cake conditions under given applied pressure, slurry concentration and viscous characteristics of filtrate.

In order to verify the validity of Eqs. (7.28) and (7.29), it should be noted that the experimental p_L-distributions have been conventionally determined as a function of the fractional distance x/L, rather than ω/ω_0. For converting ω/ω_0 into x/L, one can use the equation:

$$X/L = \int_0^{\omega/\omega_0} (1+e)\, d\left(\frac{\omega}{\omega_0}\right) \Big/ \int_0^1 (1+e)\, d\left(\frac{\omega}{\omega_0}\right) \qquad (7.30)$$

Figure 7.5 shows p_s-distributions in the cake calculated from Eq. (7.28) for various N values. As the value of N decreases, the solid compressive pressure in

the cake becomes larger. Consequently, the cake formed by non-Newtonian filtration of pseudo-plastic fluids is denser in cake structure than is the cake by usual Newtonian filtration. In Fig. 7. 6, the plot of the fractional hydraulic pressure

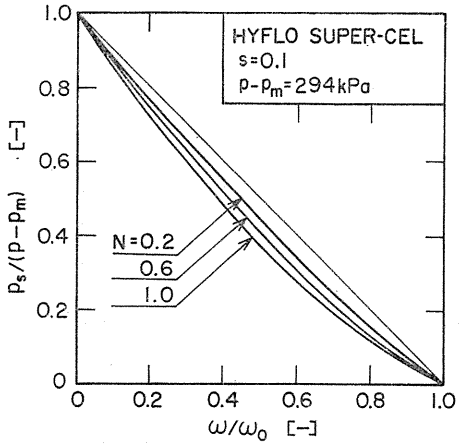

Fig. 7. 5. p_s-distributions in cake.

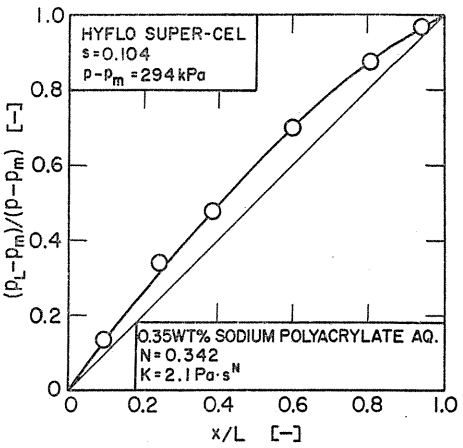

Fig. 7. 6. Hydraulic pressure distribution in cake.

drop vs. the fractional distance through the cake is shown for non-Newtonian filtration. The solid line in the figure represents the hydraulic pressure distribution calculated by Eq. (7. 28). As ε is a function of p_s as obtained from a consolidometer or from compression-permeability cell measurements, Eqs. (7. 28) or (7. 29) may be used to relate x/L to ε. In Fig. 7. 7, porosity is plotted against fractional distance through the cake. Decreasing the value of N results in a remarkable change in porosity distribution and results in a cake that is much more compact than Newtonian cake.

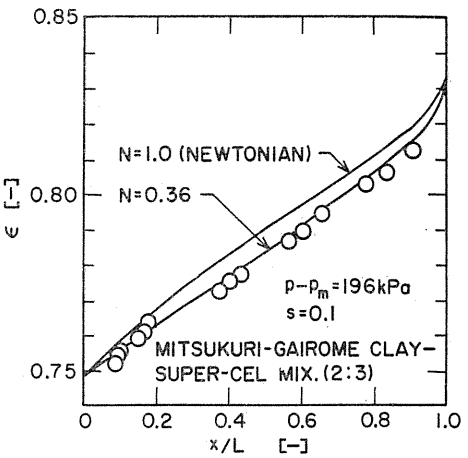

Fig. 7. 7. Porosity distributions in cake.

All the equations of non-Newtonian filtration reduce to the conventional filtration equations for Newtonian fluids by putting the flow behavior index N as unity and the fluid consistency index K as the Newtonian viscosity μ. Therefore, non-Newtonian filtration equations can be viewed as generalized filtration equations which can be applied both to Newtonian and non-Newtonian filtrations. For example, the filtration rate equation (Eq. (7. 24)) for non-Newtonian fluids reduces to Ruth's filtration relation (Eq. (1. 1)) by using Eq. (7. 16) provided the values of N and K equal unity and μ, respectively. Also, $(d\theta/dv)^N$ vs. v shows a linear relationship for non-Newtonian filtration, and $d\theta/dv$ *vs.* v is a linear relationship for Newtonian filtration.

7. 4. Filter cake deliquoring by permeation of non-Newtonian fluids

It may be seen from Figs. 7. 5 and 7. 7 that filter cakes formed from non-Newtonian filtration of pseudo-plastic fluids are much more consolidated than those from the usual Newtonian filtration, and that denser cakes are formed with decreasing value of the power-law flow behavior index N. Making use of this fact, dewatering of filter cakes can be performed by non-Newtonian permeation through cakes.[29] Constant pressure filtration experiments were conducted at pressures of 98, 196 and 294kPa. After filter cake formation was completed in the filter, non-Newtonian fluids were permeated through the filter cakes, and the percent average moisture content W of the permeated cakes was measured. The average moisture content of normal filter cakes and water-permeated cakes was also measured.

Table 7. 1. Average moisture content W of cakes under various conditions.

Filtration or permeation pressure [kPa]	Newtonian filter cake [−]	After water permeation [−]	After non-Newtonian permeation [−]	Constant pressure expression [−]
98	78.7	76.0	59.0	59.3
196	73.8	74.9	56.2	54.2
294	75.4	72.7	53.8	50.7

Slurry: Waterworks sludge (s=0.08)
Non-Newtonian fluid: 0.2 wt% sodium polyacrylate aq.
(N=0.29～0.295, K=3.91～4.0 Pa·s^N)

The values of average moisture content W of filter cakes formed under various conditions are summarized in Table 7. 1. The average moisture content of non-Newtonian permeated cakes is nearly equal to the final average moisture content of the consolidated cakes obtained by constant pressure expression. It has been demonstrated that liquid removal can be remarkably enhanced by permeation of non-Newtonian fluids through filter cakes. In the case of water permeation, there is little compaction of cakes. The experimental values of the average moisture content of non-Newtonian permeated cakes are much smaller than those of Newtonian filter cakes. In compressible cake, the absolute flow rate relative to solids in an infinitesimal layer of cake at the surface is much smaller than that at the exit. As the apparent viscosity of non-Newtonian fluids at the cake surface increases significantly in comparison with the viscosity of Newtonian fluid at the exit in the case of the permeation of highly viscous preudo-plastic non-Newtonian fluids through the cake, the filter cake is pressed by non-Newtonian fluid and the liquid is squeezed from the cake. Consequently, a remarkable dehydration of the filter cake occurs. It is supposed that a pronounced effect on dewatering occurs as the flow behavior index N decreases and the apparent viscosity increases.

8. Conclusions

The obtained results are summarized as follows:

1) Several important notes on the overall filter cake characteristics are presented.

2) The internal flow mechanism in a filter cake is examined in view of the movement of solids in cake. Taking variable flow rates of liquid and solids into account, the modern filtration theory is developed.

3) The compression-permeability test method, which is worthwhile for the analysis of internal flow mechanisms through filter cakes, is developed. Limitations of the compression-permeability cell are also discussed.

4) Porosity variations in constant pressure filtration cakes are measured by an electrical method. The experimental results show the propriety of the fundamental postulates of filtration theory.

5) Methods of solving constant rate and variable pressure-variable rate filtration problems are presented on the basis of modern cake filtration theory.

6) The non uni-dimentional filtration problems are solved in view of the effective filtration area factor j_N. Theoretical and experimental methods are presented for obtaining values of j_N for two-dimensional filtration on cylindrical surfaces and three-dimensional filtration on spherical surfaces.

7) The generalized filtration theory which can be applicable to both Newtonian and non-Newtonian fluids is developed on the basis of the power-law model of the flow of non-Newtonian fluids. The theory is applied to the problem of the filter cake dewatering.

Nomenclature

A =filter medium area [m^2]
A_E =plate area of disk-type electrode [m^2]
A_e =effective filtration area [m^2]
a =geometric constant depending on cross-sectional shape of flow path [−]
b =geometric constant depending on cross-sectional shape of flow path [−]
C =cohesive force per unit area [Pa]
C_c =empirical constant in Eq. (3.7) [−]
D =diameter of cell cylinder [m]
E =term defined by Eq. (5.4) [−]
E' =empirical constant in Eq. (3.17) [Pa$^{-\lambda'}$]
e =local void ratio [−]
e_0 =empirical constant in Eq. (3.7) [−]
e_{av} =average void ratio of entire cake [−]
$e_{av\cdot\omega}$ =average void ratio over the range from 0 to ω [−]
e_i =void ratio in infinitesimal surface layer of cake [−]
F =formation factor defined by Eq. (4.1) [−]; force [N]
F_A =apparent value of formation factor [−]
F_s =accumulated drag on the particles [N]
f =coefficient of internal friction [−]; force [N]
f_E =correction factor defined by Eq. (4.11) [−]
h =length of cylindrical filter element [m]
J =correction factor defined by Tiller and Shirato[13] [−]
J_{gen} =correction factor defined by Eq. (7.17) [−]

J_s =correction factor for the conventional Ruth's value α_R [−]
j_N =effective filtration area factor defined by Eq. (6.28) [−]
$J_{\mathrm{II,cy}}$ =effective filtration area factor for two-dimensional filtration on cylindrical surface [−]
$J_{\mathrm{III,sp}}$ =effective filtration area factor for three-dimensional filtration on spherical surface [−]
K =Ruth coefficient of constant pressure filtration [m^2/s]; fluid consistency index [$Pa \cdot s^N$]
K_0 =geometric constant defined by Eq. (7.6) [−]
K_{293} =Ruth coefficient of constant pressure filtration at 293K [m^2/s]
K_N =non-Newtonian filtration coefficient of constant pressure filtration [$m^{(1+N)/N}/s$]
k =Kozeny's constant [−]; permeability coefficient [m^2]
k_0 =coefficient of earth pressure at rest [−]
L =cake thickness [m]
m =mass ratio of wet to dry cake [−]
m_i =value of m in infinitesimal surface layer of cake [−]
N =flow behavior index [−]
n =compressibility coefficient in Eq. (3.8) [−]
p =applied filtration pressure [Pa]
p_0 =hydraulic pressure at cake surface [Pa]
p_L =local hydraulic pressure [Pa]
p_T =transmitted pressure at $z=Z$ [Pa]
p_h =horizontal compressive pressure [Pa]
p_i =low pressure below which α and ε are considered constant [Pa]; hydraulic pressure at filter medium [Pa]
p_m =pressure loss across the filter medium [Pa]
p_s =local cake compressive pressure [Pa]
p_v =vertical compressive pressure [Pa]
p_{vE} =cake compressive pressure at $z=z_E$ [Pa]
$\boldsymbol{q}$ =velocity vector of filtrate [m/s]
q =local apparent velocity of filtrate [m/s]
q_0 =apparent velocity of filtrate approaching to cake surface [m/s]
q_1 =filtration velocity [m/s]; permeation rate [m/s]
q_i =value of q in infinitesimal surface layer of cake [m/s]
R =electric resistance of cake [Ω]; viscous drag per unit volume of solids [N/m^3]
R_0 =electric resistance of filtrate [Ω]
R_A =apparent electric resistance of cake [Ω]
R_T =true local value of electric resistance in cake [Ω]
R_m =filter medium resistance [m^{-N}]
$\boldsymbol{r}$ =local apparent solid-migration velocity vector [m/s]
r =local apparent migration rate of solid [m/s]; radius [m]
r_0 =apparent migration rate of solid approaching to cake surface [m/s]; radius of cake surface [m]
r_H =hydraulic radius [m]
r_i =value of r in infinitesimal surface layer of cake [m/s]; radius of filter medium [m]
S_0 =effective specific surface of cake solids [m^{-1}]

s =mass fraction of solid in slurry [−]
T =tortuosity [−]
U =relative velocity of filtrate to solids along with the direction of filter cake depth [m/s]
U_e =velocity in actual sinuous flow path [m/s]
$\boldsymbol{u}$ =relative velocity vector of filtrate to solids [m/s]
u =apparent liquid velocity relative to solids [m/s]
u_1 =u-value at cake bottom, i. e., filtration velocity [m/s]
V_c =cake volume [m³]
v =filtrate volume per unit area [m³/m²]
v_c =cake volume per unit medium area [m³/m²]
v_m =fictitious filtrate volume per unit area, equivalent to medium resistance [m³/m²]
W =percent mass of liquid in cake [−]
W_0 =mass of dry solids in cake [kg]
w =mass of cake solids per unit area in distance x from the medium [kg/m²]
w_0 =mass of cake solids per unit area [kg/m²]
x =distance from the medium [m]
x_E =distance of electrode from the medium [m]
y =horizontal coordinate shown in Fig. 4. 12 [m]
y_0 =half distance between electrodes [m]
Z =thickness of the compressed cake [m]
z =distance from the cake surface in compression-permeability cell [m]; coordinate [m]
z_E =z-value at the position of electrode [m]

Greek symbols
α =local specific filtration resistance [m/kg]
α_R =average specific filtration resistance defined by Ruth [m/kg]
α_{av} =average specific filtration resistance [m/kg]
α_i =constant value of α when $p_s \leqq p_i$ [m/kg]
α_{op} =empirical constant in Eq. (3. 8) [$m^{1+n} \cdot s^{2n}/kg^{1+n}$]
β =empirical constant in Eq. (4. 2) [−]
β_p =empirical constant in Eq. (3. 8) [m/kg]
γ =local specific filtration resistance for power-law fluids defined by Eq. (7. 14) [m^{2-N}/kg]
γ_K =Kozicki's average specific filtration resistance defined by Eq. (7. 18) [m^{2-N}/kg]
γ_{av} =average specific filtration resistance for power-law fluids defined by Eq. (7. 16) [m^{2-N}/kg]
$\dot{\gamma}$ =shear rate [s^{-1}]
ε =local porosity [−]
ε_0 =empirical constant in Eq. (3. 6) [Pa^{λ}]
ε_1 =porosity at the interface of medium and cake [−]
ε_{av} =average porosity [−]
$\varepsilon_{av \cdot x}$ =average porosity for the portion of cake between medium and distance x [−]
ε_i =constant value of porosity when $p_s \leqq p_i$ [−]; porosity in infinitesimal surface layer of cake [−]

ζ = angle [rad]
θ = filtration time [s]
θ_m = fictitious filtration time corresponding to the medium resistance [s]
λ = exponent defined by Eq. (3.6) [−]
λ' = exponent defined by Eq. (3.17) [−]
μ = viscosity of filtrate [Pa·s]
μ_{293} = viscosity of filtrate at 293K [Pa·s]
ξ = geometric constant defined by Eq. (7.7) [−]
ρ = density of filtrate [kg/m^3]
ρ_s = true density of solids [kg/m^3]
σ = empirical constant in Eq. (4.5) [m$^{-1}\cdot\Omega^{-1}$]
τ = shear stress [Pa]
τ_w = shear stress at the wall [Pa]
ϕ = coordinate [rad]
ω = volume of cake solids per unit area up to an arbitrary position in cake [m^3/m^2]
ω_0 = volume of cake solids per unit area [m^3/m^2]

References

1) B. F. Ruth, "Studies in Filtration, Derivation of General Filtration Equations", *Ind. Eng. Chem.*, **27**, 708 (1935).
2) H. P. Grace, "Resistance and Compressibility of Filter Cakes, Part Ⅰ", *Chem. Eng. Progr.*, **49**, 303 (1953).
3) H. P. Grace, "Resistance and Compressibility of Filter Cakes, Part Ⅱ: Under Conditions of pressure Filtration", *Chem. Eng. Progr.*, **49**, 367 (1953).
4) F. M. Tiller, "The Role of Porosity in Filtration (Numerical Methods for Constant Rate and Constant Pressure Filtration Based on Kozeny's Law)", *Chem. Eng. Progr.*, **49**, 467 (1953).
5) F. M. Tiller, "The Role of Porosity in Filtration, (Part 2, Analytical Equations for Constant Rate Filtration)", *Chem. Eng. Progr.*, **51**, 282 (1955).
6) W. L. Ingmanson, "Filtration Resistance of Compressible Materials", *Chem. Eng. Progr.*, **49**, 577 (1953).
7) F. A. Kottwitz and D. R. Boylan, "Prediction of Resistance in Constant-Pressure Cake Filtration", *AIChE Journal*, **4**, 175 (1958).
8) S. Okamura and M. Shirato, "Liquid Pressure Distribution within Cakes in the Constant Pressure Filtration", *Kagaku Kōgaku*, **19**, 104 (1955).
9) S. Okamura and M. Shirato, "p_x-Distribution within Cakes in the Compression-Permeability Experiments (about Ignition-Plug Slurry)", *Kagaku Kōgaku*, **19**, 111 (1955).
10) P. C. Carman, "Fluid Flow through Granular Beds", *Trans. Instn. Chem. Engrs. (London)*, **15**, 150 (1937).
11) P. C. Carman, "Fundamental Principles of Industrial Filtration (A Critical Review of Present Knowledge)", *Trans. Instn. Chem. Engrs. (London)*, **16**, 168 (1938).
12) B. F. Ruth, "Correlating Filtration Theory with Industrial Practice", *Ind. Eng. Chem.*, **38**, 564 (1964).
13) F. M. Tiller and M. Shirato, "The Role of Porosity in Filtration: Ⅵ. New Definition of Filtration Resistance", *AIChE Journal*, **10**, 61 (1964).
14) M. Shirato, M. Sambuichi, H. Kato and T. Aragaki, "Flow Variation through Constant Pressure Filter Cake", *Kagaku Kōgaku*, **31**, 359 (1967).

15) M. Shirato, M. Sambuichi, H. Kato and T. Aragaki, "Internal Flow Mechanism in Filter Cakes", *AIChE Journal*, **15**, 405 (1969).
16) M. Shirato and S. Okamura, "Behavious of Gairome-Clay Slurries at Constant Pressure Filtration", *Kagaku Kōgaku*, **20**, 678 (1956).
17) S. Okamura and M. Shirato, "The Aging and Accuracy of the Predictions of Filtration of the Ignition-Plug Slurries", *Kagaku Kōgaku*, **20**, 98 (1956).
18) M. Shirato, T. Aragaki, R. Mori and K. Sawamoto, "Predictions of Constant Pressure and Constant Rate Filtrations Based upon an Approximate Correction for Side Wall Friction in Compression Permeability Cell Data", *J. Chem. Eng. Japan*, **1**, 86 (1968).
19) M. Shirato, T. Aragaki, K. Ichimura and N. Ootsuji, "Porosity Variation in Filter Cake under Constant-Pressure Filtration", *J. Chem. Eng. Japan*, **4**, 172 (1971).
20) M. Shirato and T. Aragaki, "Verification of Internal Flow Mechanism Theory of Cake Filtration", *Filtration & Separation*, **9**, 290 (1972).
21) M. Shirato, T. Aragaki, R. Mori and K. Imai, "Study on Variable Pressure-Variable Rate Filtration", *Kagaku Kōgaku*, **33**, 576 (1969).
22) M. Shirato, T. Murase, H. Hirate and M. Miura, "Studies in Non Uni-Dimensional Filtration——Definition of Effective Filtration Area Factor——", *Kagaku Kōgaku*, **29**, 1007 (1965).
23) M. Shirato and K. Kobayashi, "Studies in Non Uni-Dimensional Filtration, Filtration on Cylindrical, Spherical and Square Surfaces", *Memoirs of the Faculty of Engng. Nagoya Univ.*, **19**, 280 (1967).
24) M. Shirato, T. Murase and K. Kobayashi, "The Method of Calculation for Non Uni-Dimensional Filtration", *Filtration & Separation*, **5**, 219 (1968).
25) M. Shirato and T. Aragaki, "The Relations between Hydraulic and Compressive Pressures in Non Uni-Dimensional Filter Cakes", *Kagaku Kōgaku*, **33**, 205 (1969).
26) M. Shirato, T. Aragaki and S. Fujiyoshi, "Generalized Filtration Theory for Newtonian and Non-Newtonian Fluids", First World Filtration Congress, A8-1 (1974).
27) M. Shirato, T. Aragaki, E, Iritani, M. Wakimoto, S. Fujiyoshi and S. Nanda, "Constant Pressure Filtration of Power-Law Non-Newtonian Fluids", *J. Chem. Eng. Japan*, **10**, 54 (1977).
28) M. Shirato, T. Aragaki and E. Iritani, "Analysis of Constant Pressure Filtration of Power-Law Non-Newtonian Fluids", *J. Chem. Eng. Japan*, **13**, 61 (1980).
29) M. Shirato, E. Iritani, N. Hayashi and K. Ito, "Experimental Study on Filter Cake Dewatering by Permeation of Non-Newtonian Fluids", *J. Chem. Eng. Japan*, **16**, 159 (1983).
30) M. Shirato and E. Iritani, "Filtration Theory for Non-Newtonian Fluids", Proceedings of PACHEC '83, Vol. 1, 106 (1983).
31) B. F. Ruth, "Studies in Filtration, Ⅳ. Nature of Fluid Flow through Filter Septa and Its Importance in the Filtration Equation", *Ind. Eng. Chem.*, **27**, 806 (1935).
32) B. F. Ruth, "Studies in Filtration, Ⅱ. Fundamental Axiom of Constant-Pressure Filtration", *Ind. Eng. Chem.*, **25**, 153 (1933).
33) S. M. Walas, "Resistance to Filtration", *Trans. Am. Inst. Chem. Engrs.*, **42**, 783 (1946).
34) F. M. Tiller and H. R. Cooper, "The Role of Porosity in Filtration: Ⅳ. Constant Pressure Filtration", *AIChE Journal*, **6**, 595 (1960).
35) M. Shirato and M. Sambuichi, "Experimental and Theoretical Studies of Constant Pressure Filtration of Dense Slurries", *Kagaku Kōgaku*, **27**, 470 (1963).
36) E. H. Hoffing and F. J. Lockhart, "Resistance to Filtration", *Chem. Eng. Progr.*, **47**, 3 (1951).
37) K. Terzaghi, "Theoretical Soil Mechanics", p. 265, Wiley, New York (1943).
38) F. M. Tiller and H. Cooper, "The Role of Porosity in Filtration: Part Ⅴ. Porosity Variation in Filter Cakes", *AIChE Journal*, 8, 445 (1962).
39) F. M. Tiller, "The Role of Porosity in Filtration, Part 3: Variable-pressure—Variable-rate Filtration", *AIChE Journal*, 4, 170 (1958).
40) F. M. Tiller, S. Haynes, Jr. and W. M. Lu, "The Role of Porosity in Filtration: Ⅷ

Effect of Side-Wall Friction in Compression-Permeability Cells", *AIChE Journal*, **18**, 13 (1972).
41) M. Shirato, H. Kato, K. Kobayashi and H. Sakazaki, "Analysis of Settling of Thick Slurries due to Consolidation", *J. Chem. Eng. Japan*, **3**, 98 (1970).
42) M. Shirato, T. Murase, E. Iritani and N. Hayashi, "Cake Filtration-A Technique for Evaluating Compression-Permeability Data at Low Compressive Pressure", *Filtration & Separation*, **20**, 404 (1983).
43) R. L. Baird and M. G. Perry, "The Distribution of Porosity in Filter Cakes", *Filtration & Separation*, **4**, 471 (1967).
44) K. Rietema, "Stabilizing Effects in Compressible Filter Cakes", *Chem. Eng. Sci.*, **2**, 88 (1953).
45) G. E. Archie, "The Electrical Resistivity Log as an Aid in Determining Some Reservoir Characteristics", *Trans. AIME*, **146**, 54 (1942).
46) H. Brenner, "Three-Dimensional Filtration on a Circular Leaf", *AIChE Journal*, **7**, 666 (1961).
47) J. I. Leonard and H. Brenner, "Experimental Studies of Three-Dimensional Filtration on a Circular Leaf", *AIChE Journal*, **11**, 965 (1965).
48) G. P. Tschebotarioff, "Soil Mechanics, Foundations, and Earth Structures", p. 235, McGraw-Hill Book Co., Inc., New York (1951).
49) F. M. Tiller and C. J. Huang, "Theory of Filtration Equipment", *Ind. Eng. Chem.*, **53**, 529 (1961).
50) R. E. Collins, "Modern Chemical Engineering", Vol. 1, Physical Operations, p. 328, Reinhold (1962).
51) W. Kozicki, C. Tiu and A. R. K. Rao, "Filtration of Non-Newtonian Fluids", *Can. J. Chem. Eng.*, **46**, 313 (1968).
52) W. Kozicki, A. R. K. Rao and C. Tiu, "Filtration of Polymer Solutions", *Chem. Eng. Sci.*, **27**, 615 (1972).
53) M. Shirato, T. Aragaki and E. Iritani, "Blocking Filtration Laws for Filtration of Power-Law Non-Newtonian Fluids", *J. Chem. Eng. Japan*, **12**, 162 (1979).
54) M. Shirato, T. Aragaki, E. Iritani and T. Funahashi, "Constant Rate and Variable Pressure-Variable Rate Filtration of Power-Law Non-Newtonian Fluids", *J. Chem. Eng. Japan*, **13**, 473 (1980).
55) W. Kozicki, C. J. Hsu and C. Tiu, "Non-Newtonian Flow through Packed Beds and Porous Media", *Chem. Eng. Sci.*, **22**, 487 (1967).
56) M. Shirato, T. Murase, M. Negawa and H. Moridera, "Analysis of Expression Operations", *J. Chem. Eng. Japan*, **4**, 263 (1971).